

**WIRELESS POWER TRANSFER VIA MAGNETICALLY COUPLED
RESONANCE FOR SMALL ELECTRONIC DEVICES**

by

Wan Peng

Submitted in partial fulfilment of the requirements

for the degree of Master of Applied Science

at

Dalhousie University

Halifax, Nova Scotia

April 2018

© Copyright by Wan Peng, 2018

TABLE OF CONTENTS

| | |
|--|------|
| LIST OF TABLES | vi |
| LIST OF FIGURES | vii |
| ABSTRACT | x |
| LIST OF ABBREVIATIONS USED..... | xi |
| ACKNOWLEDGMENTS..... | xiii |
| CHAPTER 1 INTRODUCTION..... | 1 |
| 1.1 Motivation..... | 1 |
| 1.2 Research Objectives..... | 3 |
| 1.3 Contributions..... | 4 |
| 1.4 Thesis Organization..... | 5 |
| CHAPTER 2 BACKGROUND AND LITERATURE REVIEW..... | 7 |
| 2.1 Introduction to Wireless Power Transfer (WPT)..... | 7 |
| 2.1.1 Configuration..... | 8 |
| 2.1.2 Classification..... | 11 |
| 2.1.3 Applications..... | 12 |
| 2.1.4 Challenges..... | 14 |
| 2.1.5 Standards..... | 15 |
| 2.2 Near-Field Wireless Power Transfer Techniques..... | 16 |
| 2.1.1 Inductive Coupling..... | 16 |

| | |
|---|----|
| 2.2.2 Magnetically Coupled Resonance..... | 18 |
| 2.3 Far-Field Wireless Power Transfer Techniques..... | 22 |
| 2.3.1 Microwave Radiation..... | 22 |
| 2.3.2 Laser Beaming..... | 23 |
| 2.4 WPT for Small Electronic Devices..... | 25 |
| 2.5 Auxiliary Materials | 29 |
| 2.6 WPT Using MCR for Small Electronic Devices..... | 32 |
| 2.6.1 Coil Structures..... | 32 |
| 2.6.2 Coil Shapes..... | 35 |
| 2.6.3 Planar MCR-WPT for 13.56 MHz Applications..... | 35 |
| 2.7 Summary..... | 37 |
| CHAPTER 3 OUR DESIGN METHODOLOGY..... | 39 |
| 3.1 Theoretical Analyses..... | 39 |
| 3.2 Ferrite Materials..... | 43 |
| 3.3 Finite Element Method..... | 44 |
| 3.4 Summary..... | 45 |
| CHAPTER 4 THE PLANAR SYMMETRIC PLANAR MCR-WPT SYSTEM..... | 47 |
| 4.1 Design..... | 47 |
| 4.1.1 Design Parameters..... | 47 |
| 4.1.2 The Proposed System..... | 53 |
| 4.2 Result..... | 54 |

| | |
|---|----|
| 4.3 Summary..... | 59 |
| CHAPTER 5 THE PLANAR ASYMMETRIC PLANAR MCR-WPT SYSTEM..... | 61 |
| 5.1 Design..... | 61 |
| 5.1.1 Efficiency Improvement by Auxiliary Strips..... | 61 |
| 5.1.2 The Proposed System..... | 63 |
| 5.2 Results..... | 66 |
| 5.3 Effects of Conductive Object And Shielding Ferrite..... | 72 |
| 5.3.1 Effects of Conductive Objects | 72 |
| 5.3.2 Effects of Shielding Ferrite Sheet | 75 |
| 5.4 Summary..... | 81 |
| CHAPTER 6 CONCLUSION AND FUTURE WORK..... | 83 |
| 6.1 Conclusion..... | 83 |
| 6.2 Future Work..... | 84 |
| REFERENCES..... | 86 |

Dedication

To the memory of my mother X. Yan and to my beloved father F. Peng

LIST OF TABLES

| | |
|---|----|
| Table 2-1: Comparison of the main WPT technologies..... | 11 |
| Table 4-1: Design parameters for symmetric MCR-WPT system..... | 52 |
| Table 4-2: The simulated results of S_{21} parameter with or without ferrites | 57 |
| Table 5-1: Design parameters for asymmetric MCR-WPT system | 65 |
| Table 5-2: Simulated power transfer efficiency with different turns of the receiver PSC and in the presence of auxiliary strip presented or not..... | 67 |
| Table 5-3: Summing up different ferrite sizes and functions | 81 |

LIST OF FIGURES

| | |
|---|----|
| Figure 2-1: Elements of WPT systems..... | 9 |
| Figure 2-2: Block diagram of inductive coupling..... | 17 |
| Figure 2-3: Schematic of the MCR-WPT system..... | 19 |
| Figure 2-4: Three conditions of MCR-WPT technique..... | 21 |
| Figure 2-5: Block diagram of microwave power transfer..... | 23 |
| Figure 2-6: The laser fundamentals..... | 24 |
| Figure 2-7: Schematic of distributed laser charging..... | 25 |
| Figure 3-1: Equivalent circuit model of the planarized MCR-WPT system..... | 40 |
| Figure 4-1: The proposed ferrite-less symmetric WPT system transmitter and receiver; (a) front view, (b) back view, (c) Partial view of a corner..... | 49 |
| Figure 4-2: The Ferrite structures being used for the proposed symmetric MCR-WPT system; (a) central ferrite core, (b) bottom ferrite plate | 50 |
| Figure 4-3: Structure of the proposed ferrites combined symmetric WPT system transmitter and receiver; (a) front view, (b) back view, (c) side view | 51 |
| Figure 4-4: S_{21} versus sizes of central ferrite with the symmetric WPT system..... | 53 |
| Figure 4-5: Overview of the proposed symmetric WPT system..... | 54 |
| Figure 4-6: The conventional WPT system and its test setup... .. | 55 |
| Figure 4-7: The proposed system with the ferrite structures and its test setup..... | 55 |
| Figure 4-8: The conventional and the proposed WPT receivers in size comparison of | |

| | |
|---|----|
| iPhone 6s... | 56 |
| Figure 4-9: Measured and simulated transfer efficiency of the symmetric WPT system with or without ferrite with 35 mm air gap..... | 58 |
| Figure 4-10: Measured power transfer efficiency of the proposed symmetric WPT system with ferrites when the distance between the transmitter and the receiver is changed from 10 mm to 80 mm..... | 59 |
| Figure 5-1: Measured $ S_{21} $ of the proposed asymmetric WPT system receiver with and without auxiliary strip at the distance of 60 mm between the transmitter and receiver. ... | 62 |
| Figure 5-2: Geometry of the proposed asymmetric WPT system transmitter; (a) front view and (b) back view | 63 |
| Figure 5-3: Structure of the proposed asymmetric WPT system receiver; (a) front view, (b) back view..... | 65 |
| Figure 5-4: Overview of the proposed asymmetric WPT system | 66 |
| Figure 5-5: The optimized asymmetric WPT system and the test setup.... | 68 |
| Figure 5-6: The measured $ S_{11} $ and $ S_{21} $ of the optimized asymmetric WPT system at 13.56 MHz with the distance of 60 mm between the transmitter and receiver..... | 69 |
| Figure 5-7: Measured and simulated power transfer efficiency of the proposed asymmetric WPT system at 13.56 MHz with 60 mm air gap..... | 70 |
| Figure 5-8: The S_{21} performance when directional misalignment of the optimized asymmetric WPT system..... | 71 |
| Figure 5-9: Experiment of lighting up an LED bulb wirelessly using the proposed | |

| | |
|---|----|
| asymmetric system | 72 |
| Figure 5-10: Headsets-sized metal sheet representing the back cover of a cell phone; (a) with the camera hole in the middle, (b) with the camera hole and the vertical slot. | 74 |
| Figure 5-11: Induced eddy current on the metal sheet, (a) without vertical slot, (b) with vertical slot. | 74 |
| Figure 5-12: Electromagnetic field distribution when ferrite sheet placed near asymmetric WPT system or not; (a) without ferrite sheet, (b) with ferrite sheet..... | 76 |
| Figure 5-13: Measurement set up to test influences of the ferrite sheet on the asymmetric WPT system: (a) front view and (b) over view..... | 77 |
| Figure 5-14: Measurement set up to test the influences of ferrite sheet on the asymmetric WPT system; (a) front view and (b) over view... .. | 78 |
| Figure 5-15: Measurement set up to test the effects of both metal (aluminum) and ferrite sheets placed behind the receiver..... | 79 |
| Figure 5-16: The measured $ S_{11} $ of the proposed asymmetric WPT system with ferrite or aluminum sheet near the receiver. | 80 |
| Figure 5-17: The measured transfer efficiency of the proposed asymmetric WPT system with ferrite or aluminum sheet or both nearby the receiver in comparison with the receiver only. | 80 |

ABSTRACT

The widespread use of all kinds of small portable devices including cell phones have created the demands for wireless power transfer (WPT) systems that are proper for small size mobile devices. Most of the existing systems developed in the past decade are large compared to mobile phones. For those small size WPT systems, power transmitting distances are very limited and the receivers need to be placed in proximity with the transmitters or even require contact. Moreover, ferrimagnetic materials have been investigated in several papers to improve wireless charging system performances. However, there are few published works that effectively incorporate different ferrite structures with various functions.

In this thesis, magnetically coupled resonance (MCR) WPT systems are developed with innovative design techniques. Specifically, two MCR-WPT systems are proposed: one is symmetric while another is asymmetric. The symmetric system has a small transmitter of the same size as the receiver of $32 \times 32 \times 3.91$ mm. The optimal charging distance is 35 mm with the maximum transfer efficiency of 32.8%. The asymmetric system has a large transmitter of $200 \times 200 \times 1.6$ mm and the receiver size remains small. The maximum transfer efficiency is 51.8% and the optimal charging distance is 60 mm.

The proposed systems are first simulated using the finite element method, and then fabricated and tested. The results demonstrate that the proposed systems can enable wireless power charging of small electronics with acceptable efficiency.

LIST OF ABBREVIATIONS AND SYMBOLS USED

WPT – Wireless Power Transfer

MCR – Magnetically Coupled Resonance

PSC – Printed Spiral Coil

EM – Electromagnetic

EMF – Electromagnetic Field

EMI – Electromagnetic Interference

R – Resistance

L – Inductance

C – Capacitance

Z – Impedance

M – Mutual Inductance

Q – Quality Factor

DC – Direct Current

AC – Alternating Current

RF – Radio Frequency

I – Current

V – Volt

Hz – Hertz

KHz – Kilohertz

MHz – Megahertz

W – Watt

kW – Kilowatt

d – Distance

η – Transfer Efficiency

f – Frequency

ω – Angular Frequency

RFID – Radio Frequency Identification

m – Meter

mm – Millimeter

H – Henry

S – Siemens

μ_r – Relative Permeability

σ – Conductivity

nF – Nano Farad

pF – Pico Farad

dB – Decibel

HFSS – High Frequency Structure Simulator

ACKNOWLEDGEMENTS

First, I sincerely wish to thank my supervisor, Prof. Zhizhang (David) Chen, who gave me the opportunity to join his group, and let me work on various projects. It was a real pleasure for me to work under his supervision, and it was my honor to be his M.Sc. student.

I also want to thank my colleagues, Zhu Liu, Wei Fan and Farid Jolani, for their valuable discussions and suggestions during my projects as well as my Master studies. I am immensely grateful to them. They inspired me with their brilliant ideas and novel concepts.

Furthermore, I would like to thank my committee members, Dr. Sergey Ponomarenko and Dr. William J. Phillips, for their reviews of my thesis and their constructive comments and feedbacks.

I would also like to say thank you to Nicole Smith and Mary Little in the department office for their friendly help on day-to-day matters.

Special gratitude goes to my dearest friends, Weiyi Li, Qingqing Li, Jie Zhang and my boyfriend Deyu Li for always being supportive.

Finally, I want to thank my parents, Feng Peng and Xiangtao Yan, for supporting me studying abroad and for their deep loves.

CHAPTER 1 INTRODUCTION

1.1 Motivation

Nowadays, we are surrounded by all kinds of electronic devices ranging from relatively large size apparatuses, such as household appliances, automobiles and industrial equipment, to handheld mobile devices including laptops, tablets and cell phones. All these electronic devices need continuous power supply or batteries for limited periods of use, which make the device tethered by a cable or wire. Most people have suffered from disruptions in use when their mobile devices ran out of battery and no power plugs or wires nearby can be found to recharge immediately. On the other hand, the advanced wireless communication and semiconductor technology has enabled smaller and smaller mobile devices; as a result, charging wires has become redundant and inconvenient. To address the issue, the wireless power transfer (WPT) concept has become attractive.

The WPT concept is used to transfer electric power without any physical connections. In the 19th and early 20th century, before the electrical wire grids, Nikola Tesla devoted much effort toward schemes to transport power wirelessly. The Tesla coil is a well-known invention by him for long-range wireless power transmission [1]. Since then, a wide range of WPT techniques have been explored and reported, in particular after recent surges with uses of numerous autonomous electronic devices (robots, electric vehicles, laptops, cell phones, etc.). The WPT overcomes the shortcomings that traditional wired power transfer methods have: cable abrasion, electric spark, noise generation, and mechanical damages

[2].

There are many WPT methods developed and each of them is developed based on different applications and design requirements. However, in general, they can be classified into four major types: inductive, magnetically coupled resonance, microwave radiation and laser beaming.

Inductive power transfer is the most commonly used WPT method based on Faraday's law of electromagnetic induction. It works in the way that alternating electromagnetic (EM) energy in a transmitter excites EM energy that is magnetically coupled to a receiver. Magnetically coupled resonance (MCR) is the second method where a transmitter and a receiver resonate at the same preselected frequency and then magnetically coupled for power transfer. Both the transmitter and receiver have capacitive components to adjust the resonant frequencies to be the same. Microwave radiation and laser beaming are the long-range power transfer methods which use electromagnetic radiation or laser to carry power over a long distance. The MCR method presented longer transmission distance than the inductive coupling and higher efficiency than the far-fields methods [2]-[3]. Thus, the MCR is the subject of this thesis for intermediate-distance wireless power transfer.

Different MCR-WPT systems have been proposed for recharging electric vehicles [4], [5] and [6], laptop computers [3] and [7] and medical devices [8] and [9]. For portable electronic devices, [3] reports a WPT system that has a power transfer efficiency of 50% at a distance of 0.7 m; the radius of the receiver coil is 30 cm which is bulky for tablets and cell phones. In [10], a WPT system for cell phones was proposed but the system is

complex and hard to produce in a large quantity. Some other planarized designs are demonstrated in [11]-[15] with good performances but their sizes are still too large to be used for mobile phones. An effective WPT method is needed to make electronic devices completely mobile without redundant cable or wire connection, especially for those commonly used small size consumer electronic devices like mobile phones. In addition, some implantable medical devices such as cardiac pacemakers are in need of wireless recharging via human body and air gap to avoid surgical operations [8].

Magnetic materials, such as metamaterials and ferrimagnetic materials (i.e., ferrites), are used in WPT system designs. Ferrites are known to be capable of confining and leading magnetic flux; thus, they are investigated for use in WPT systems to improve system performances [16]-[20]. Several other design techniques such as frequency tracking [3], additional relay coil [21] and multilayer transmitter and receiver [13] are proposed and applied to solve the challenges facing the WPT systems. The search for better and more practical wireless charging systems has been conducted unabatedly.

1.2 Research Objectives

The primary goal of this thesis is to develop a novel WPT system for charging small electronic devices with receiver size smaller than a typical smart phone and overcome the disadvantages of the existing WPT systems have such as limited charging distance. This research is a continuation of the previously published work of our research group [11]-[13], and the specific research objectives are as follows:

- 1) To study planar four-coil MCR-WPT systems and their performances with small receiver sizes. This objective is to assess the effects of geometrical parameters (such as the width and turns of the printed spiral coil (PSC)) and electrical parameters (such as self-inductance (L), mutual inductance (M), quality factor (Q)) on power transfer efficiency.
- 2) To develop easy-to-implement, low-profile and fully planar symmetric and asymmetric MCR-WPT systems for different applications. They are simulated, prototyped and tested for their feasibility and performances.
- 3) To research different ferrite components and configurations and to understand how they can be used to improve the proposed WPT system performances.

1.3 Contributions

This thesis contributes to the state of the art in the following ways:

- 1) A planar symmetric MCR-WPT system is proposed, with both transmitter and receiver size equal to 32 mm^2 ; it is much smaller than most of the existing systems. Two ferrite components are incorporated into the system to effectively improve the power transfer efficiency.
- 2) A planar asymmetric MCR-WPT system with the receiver size of 32 mm^2 and the transmitter size of 200 mm^2 is proposed. Two different ferrite component structures are used to improve the power transfer efficiency. The directional misalignment performance is investigated as well.

- 3) Effects of ferrite and conductive materials, such as aluminum, on the asymmetric MCR-WPT system performance are investigated. Possible solutions for mitigating influences of nearby conductive materials for the WPT systems are presented.
- 4) Three different ferrite configurations are studied and summarized for future applications.

1.4 Thesis Organization

This thesis is divided into six chapters, together with the abstract and list of references. The contents in each chapter are summarized as follows.

Chapter 1 presents the motivation, research objectives, contributions and organization of the thesis. Chapter 2 provides the general review of the state-of-the-art. General system configurations, classification, practical applications and the main challenges are introduced. Chapter 3 describes the WPT systems without ferrites and their equivalent circuit models. Chapter 4 and 5 present the designs and test results of the proposed MCR-WPT systems. They are optimized, fabricated and then compared. More specifically, a planar symmetric MCR-WPT system is proposed in Chapter 4 with the dimension of the transmitter and receiver smaller than a typical cell phone. Two ferrite components are incorporated to improve system performances. Chapter 5 shows the asymmetric MCR-WPT system. An auxiliary strip is employed to improve the power transfer efficiency. Adjustment of system structures based on the symmetric system is made to improve the maximum power transfer efficiency as well as to extend transmission distance. The optimized system is fabricated,

and the measurement results presented. Ferrite and metallic sheets are investigated for their influences on the system performances. Chapter 6 draws the conclusions and presents the future directions for wireless charging systems used for small electronic devices.

CHAPTER 2 BACKGROUND AND LITERATURE REVIEW

In this chapter, background and literature review of the WPT systems are presented. A brief introduction to the WPT concept, system configurations, applications and challenges is given at first, followed by the details of four classifications of the WPT systems. The WPT systems used for small electronic device applications and the MCR method are then further discussed including the recent works.

2.1 Introduction to the Wireless Power Transfer (WPT)

From a practical point of view, WPT is to wirelessly transfer electric power without any physical connection from a power source to an electrical load such as an electrical power grid or an appliance. From the theoretical point of view, WPT is to deliver energy carried in a time-varying electromagnetic field from a power transmitting unit to a power receiving unit through a dielectric media such as air and water.

Based on this WPT concept, all types of battery or plug-in charging devices can be powered and recharged wirelessly when being aligned to a wireless charging transmitter and placed nearby. The WPT concept has become popular these years for its convenience, reliability and safety. Current power supply systems such as plugs or batteries can suffer from mechanical damages and mismatching with wrong connections.

So far, many commercial products have been developed with the capability of being

wirelessly charged. The newly released iPhone 10 has the wireless charged capability. Tesla is promoting automobile wireless charging systems. The Mercedes-Benz S550e plug-in hybrid will add a wireless charging system in year 2018. Dell also released the Windows 10 laptop with intrinsic wireless charging function. Experts predicted that Apple and Tesla, as the industrial leaders of consumer electronics and automobiles respectively, will lead the trend with their efforts for wireless charging [22].

The configuration, classification, applications and challenges of WPT systems are discussed in the following sections.

2.1.1 Configuration

Many WPT systems have been developed over the past few decades [4, 5, 10, 23, 24]. Figure 2-1 shows a typical WPT system for low power consumer electronics. A complete WPT system consists of the following components: the power source, power transmitting unit (or wireless charging transmitter), power receiving unit (or wireless charging receiver), electrical load and peripheral circuits.

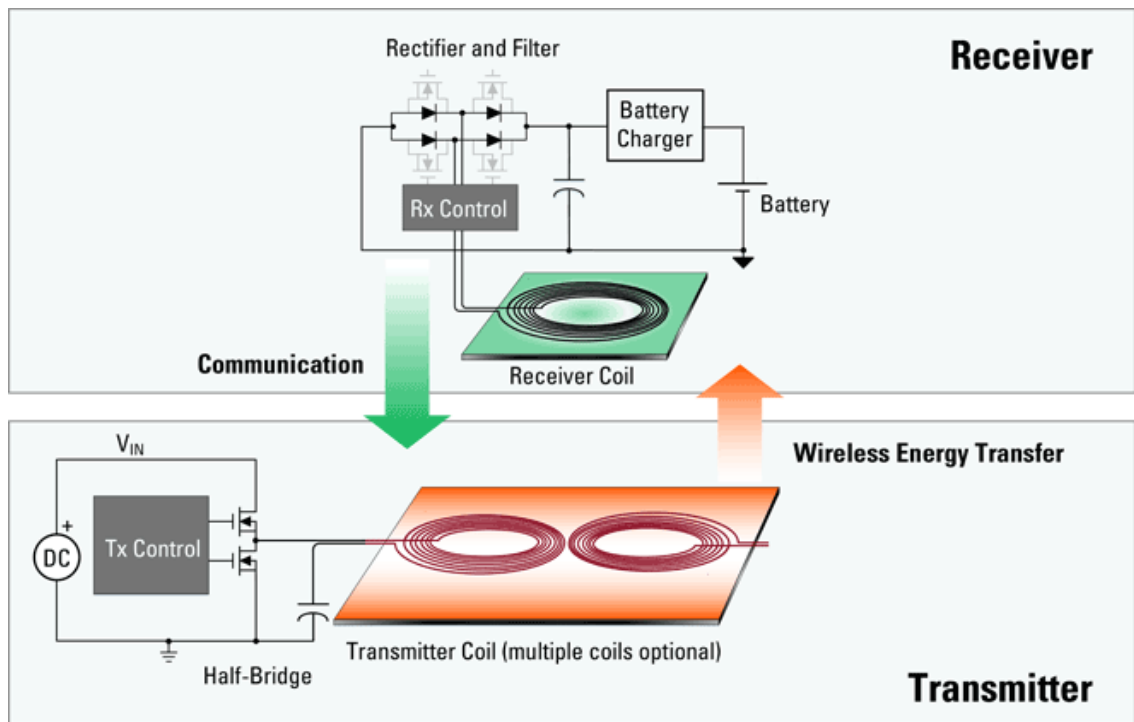


Fig 2-1: Elements of WPT systems [22]

Figure 2-1 shows a typical charging transmitter biased by a 5 - 19 V direct current (DC) power. The DC power may come from the rectification of the 50 or 60 Hz alternating current (AC) power available in most buildings. The transmitting coils driven by an H-bridge circuit consists two or four field-effective transistors with a serial connected capacitor through which an intrinsic resonant frequency is achieved.

A WPT system comes with a transmitter coil that delivers wireless power to the receiver coil. A coil array can also be used [15] and each coil is driven by an H-bridge. The power is delivered over space to the receiver that has the similar structure as the transmitter does. Diodes or transistors are then used to rectify the receiving power and to have the highest possible power transfer efficiency. Then the power is being filtered by capacitors

as well as other adjusting components and finally is transferred to batteries or loads. The charging process starts when the batteries or electrical loads inside portable devices begin receiving energy.

One of the most desirable features for wireless charging is that multiple electronic devices can be charged at the same time with a single power transmitter. It is achieved using multiple transmit coils or coil arrays in a transmitter. The transmitter in Figure 2-1 is an example for multi-receiver charging using coil arrays. In [15], both 2×2 and 3×3 transmitter arrays were designed and fabricated to charge a Bluetooth speaker, a smartphone and LED table lamps at the same time. Another 2×2 transmitting coils configuration was presented in [25] with hardware validation. [26] explored the multiple charging potentials using resonant coupling mechanism and validated them through lighting two LEDs simultaneously with the same transmitter. The main challenges for multi-receiver charging WPT systems are that the power achieved by each receiver is divided from the same power source, leading to the decrease of power transfer efficiency in comparisons with a single receiver. In other words, to achieve the same power transfer efficiency, a much higher power level is needed from the transmitter in the multi-receiver WPT systems. Another challenge is that the output power and the end-to-end power transfer efficiency is dependent on the loads [25].

The focus of this work is the design of the transmitter and receiver coil components. The peripheral circuits such as rectifiers, filters and converters are not the scope of this thesis.

2.1.2 Classification

Many WPT techniques have been proposed and developed. They can be classified into four categories based on the WPT methods. The four methods are inductive coupling, magnetic coupled resonance, microwave radiation and laser beaming. They are summarized in Table 2-1.

Table 2-1: Comparison of the main WPT technologies [16]

| | Efficiency | Distance | Mobility | Safety |
|---------------------------------------|-------------|-----------------------------|-----------------------|-------------------------------------|
| Inductive Coupling | High | Short | Bad | Safe |
| Magnetically Coupled Resonance | High | Short - Middle | To Some Extent | Safe |
| Microwave radiation | Low | Long | Good | Safety Constraints May Apply |
| Laser Beaming | High | Long (Line of Sight) | To Some Extent | Safety Constraints May Apply |

In terms of the power transfer distance, WPT techniques can be grouped into two categories, near field (also called non-radiative) and far-field (also called radiative). In non-radiative techniques, power is transferred by magnetic fields using inductive coupling between coils of wire, or by resonant coupling between power transmitting and receiving units. The former is the most commonly used wireless technology not only presented in academic papers including [4, 5, 10, 23, 24] but also available in commercial products such as electric toothbrush chargers. The latter is a mid-range non-radiative coupling method

whose transmission distance is greater than inductive coupling. It uses the resonant coupling with both the transmitting and receiving coils tuned at the same resonant frequency. This method has been investigated and developed for charging electric vehicles [27], medical implantable devices [8], and small handheld electronic devices [28].

In the far-field or radiative techniques, also called power beaming, power is transferred by beams of electromagnetic radiation such as microwave or laser beams. These techniques can transport energy at a much longer distance. However, for the laser beaming method, the receiver must be aimed at the transmitter in the line of sight, while for the microwave radiation, the underlying safety issue for a human body cannot be neglected. Their applications include solar power satellites and wireless powered drone aircraft.

The fundamental theories of four main wireless charging techniques, their charging distance, features, pros and cons, as well as applications are discussed in [29]-[31]. This thesis focuses on magnetically coupled resonance (MCR) since its advantages include high charging efficiency and relatively long transmission distance. The applications under consideration are the charging of small consumer electronics, especially mobile phones.

2.1.3 Applications

The WPT techniques can be widely applied to charge electronic devices and systems. The existing products and systems as well as potential applications can be categorized as follows:

- Applications to small consumer electronics such as smart phones [10, 28, 33], portable

multimedia players such as Bluetooth amplifier, digital cameras, tablets, computers [3, 7] and wearable electronic devices [34, 35]. Consumers are continually looking for easy and user-friendly solutions that can provide free charging space and less charging time. The power level for these applications is between 2 W and 15 W. The communications between the transmitter and the receiver are needed to negotiate the charging specifications such as start and stop charging as well as charging voltage.

- Applications to wireless accessories such as wireless headsets, speakers, mice and keyboards. These accessories are less aware by public for the needs of wireless charging but they could have wireless charging functions. With the continuously shrinking sizes, charging coils should be small enough to be implantable in these devices. Many of accessories need to be mechanically sealed well for waterproof which presents the challenges for wired charging; therefore, WPT is a good means for the charging.
- Development of public-access charging terminals. They can be used in public places such as cafeterias, airports and hotels. They can be incorporated into furniture with products such as charging pads attached under the tables. Safety issues should be taken into consideration when deploying such charging pads in public areas.
- Charging of electric vehicles such as cars and autonomous unmanned vehicles [4, 6, 27]. High power is needed for this application and both inductive and magnetically resonant coupling are employed for they can provide high-power and short-distance power transfer.

- Recharging of medical implanted devices [8], [9]. Many devices have been and will be implanted into human bodies. They require constant power supply and replacements of battery if needed. Such a replacement often asks for surgery that may lead to health risks and even life safety. Wireless charging provides a means to avoid the problem.

2.1.4 Challenges

There are three main factors to be considered in developing WPT systems. First, power transfer efficiency normally decreases with the increase of the distance between a transmitter and a receiver. Secondly, power transfer efficiency normally decreases with lateral or angular misalignment between a transmitter and a receiver. Finally, electromagnetic radiation and interferences generated by a WPT system may lead to safety concern.

Power transfer efficiency is the most important specification for a wireless charging system. Power transfer distance and misalignments between transmitter and receiver are the key measures for feasibility and convenience of a WPT system. In most of the cases, the transfer or transmission distance and efficiency of a WPT system are inversely square relation as shown in equation (2-1).

$$\frac{1}{d^2} \propto \eta \quad (2-1)$$

where d is the transmission distance, η is the transfer efficiency.

Many efforts have been made to address the above-mentioned problems. A transmitting coil array structure has been presented in [15] to mitigate axial and lateral misalignment

problems. The results show that the transfer efficiency is fairly stable when the receiver moves in a plane or rotates around the central point. A minimum of 65% power transfer efficiency can be achieved [15].

Shielding materials such as ferrite and aluminum have been used to deal with the electromagnetic interference and leakage problems in [16]-[20]. The systems developed with shielding materials can efficiently control unwanted electromagnetic fields and concentrate power within the areas covered by the transmitter and the receiver.

2.1.5 Standards

Given the different WPT systems using for different power and voltage levels and operating frequencies, certain WPT standards have been studied and proposed by various organizations. The most well-known ones are the ‘Qi’ standard, proposed by the so-called Wireless Power Consortium. This standard regulates issues for WPT systems and lists, but not restricted to, alignment approaches, categories of power requirements and interoperable wireless charging formats [30, 36]. Circuits and systems with this standard are proposed such as those presented in [9, 25, 36]. The history, specifications and outlook for the ‘Qi’ standard can be found in [37].

Another standard was proposed by the Alliance for Wireless Power (A4WP). It operates at 6.78 MHz and uses the magnetically resonance coupling scheme [36]. The WPT systems using this standard have been developed such as those described in [9] and [38].

Theses WPT standards are used to regulate different wireless charging solutions for

charged objects. Taking a mobile phone as an example, the WPT standards should allow wireless charging techniques applied to mobile phones of most brands [37].

The WPT standard is one of the important factors that should be taken into consideration in a WPT system design process to obtain a more practical and compatible system. This paper considers 13.56 MHz of industrial, scientific and medical (ISM) band that is widely used for radio frequency identification (RFID) under the 'Qi' standard.

2.2 Near-Field Wireless Power Transfer Techniques

Near-field WPT techniques are also known as non-radiative WPT methods. They usually use magnetic coupling instead of radiative electromagnetic waves to transfer wireless energy. They are also being applied in nearer distances compared to the far-field or radiative methods. This type of WPT technique can be used to benefit power utilities such as cell phones [10, 28, 33], high power transportation applications [4, 6, 27] and RFID. Inductive coupling and resonant coupling are the most common WPT methods in this type.

2.2.1 Inductive Coupling

Inductive coupling is a widely used wireless charging method which has been applied in many products on the market. The theory is based on Faraday's induction law which says that time-varying electromagnetic field generates time-varying electric current. Figure 2-2 is a common block diagram of an inductive coupling WPT system. In the area enclosed by dashed lines, the transmitting coil on the left is driven by time-varying current which in

turn induces time-varying magnetic fields; they pass through the receiving coil on the right over the air gap and excite time-varying electric current in the receiving coil. Hence, power is delivered from the transmitter to the receiver through air space without wire connection.

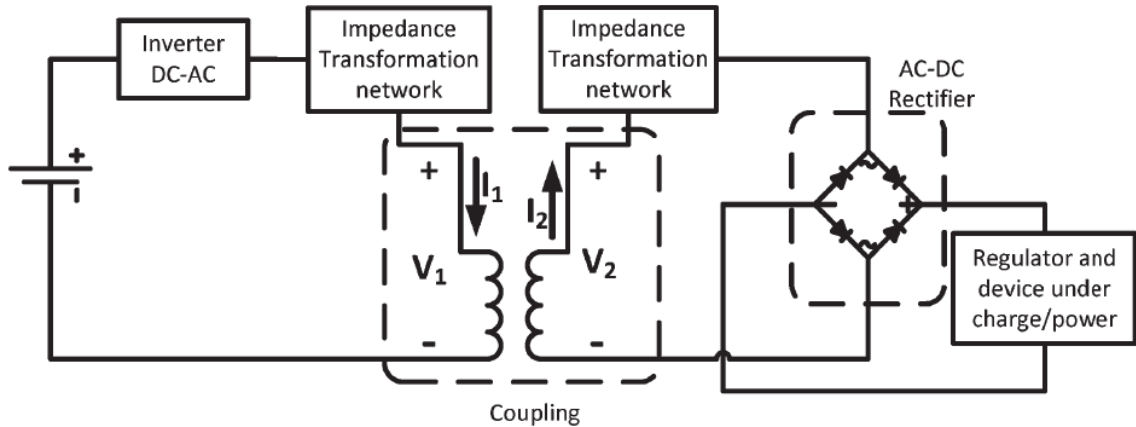


Figure 2-2: Block diagram of inductive coupling [40]

Inductive coupling is a major candidate of WPT systems and much work has been done along this line. The inductive coupling WPT system presented in [10] for cell phone charging was able to achieve 90% transfer efficiency with the power level between 6.8 W to 8.2 W. Wireless charging of electric vehicles is demonstrated in [4], [23] and [39]. The highest efficiency was 74% [39] and up to 20 kW power could be transferred [23].

The inductive coupling WPT systems have been commercialized by Apple and Tesla. iPhone 10 and electric tooth brush were wireless-charging enabled with simple implementation and high efficiency. The drawback is that the charged devices are required to be tightly aligned with the transmitters within several millimeters (usually 5 mm), which greatly degrades mobility. Moreover, inductive coupling is easily affected by surrounding conductive objects that could cause heat generation which is hazardous and unwanted.

2.2.2 Magnetically Coupled Resonance

The magnetically coupled resonance (MCR, also named magnetic resonance) WPT is a method that becomes increasingly popular for short- to middle-range wireless charging. It is chosen as the WPT method in this work, due to its extended transmission distance and suitability for portable electronic device application as mentioned in Section 1.1. Magnetically coupled resonant WPT has greater power transmission distance than the inductive coupling method due to its magnetic resonance mechanism.

A typical MCR-WPT system consists four coils, a driving loop and a transmitting resonator on the transmitter side and a receiving resonator and a load loop on the receiver side as shown in Figure 2-3. The driving loop is driven by an electric source while the load loop is connected to the object to be charged. The resonators are regarded as two RLC tank circuits; they can be self-resonant or capacitive loaded. The differences and comparisons of these two topologies were given in [41]. A self-resonant topology can be found in [42] and the drawback is that the self-capacitances are usually small and hard to tune the resonant frequency. In addition, the resonant frequency is easily affected by external objects. The capacitive loaded one is used in this thesis since it is convenient to adjust the resonant frequency by changing the values connected to coils. There are various kinds of capacitors can be used for MCR-WPT resonators such as parallel-plate capacitors, high Q-lumped capacitor, or flexible coaxial-like capacitor [42]. The lumped capacitor is used in this thesis because it is easy to set a desired capacitance. By fine-tuning the capacitor values,

the transmitter and receiver resonators can resonate at the same frequency. Power is transferred from the driving loop to the transmitting resonator loop through inductive coupling, and is magnetically coupled to the receiving resonator and then inductively coupled to the load loop, thus achieving power transfer from one point to another through an air gap.

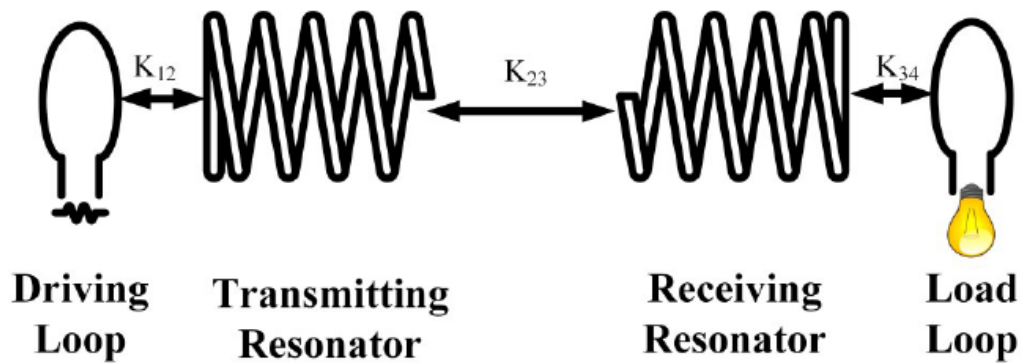


Figure 2-3: Schematic of the MCR-WPT system [41]

The MCR-WPT concept was first introduced by a research group from MIT, it was able to transfer 60 W with 40% efficiency over distances more than 2 m [1]. This method then gained attention in the following decade because of its intrinsic advantages that its resonant coupling feature makes the energy transfer more efficient over a larger distance compared to inductive coupling. Once the system has been optimized, a typical MCR-WPT system can achieve a transmission distance several times of the coil size with a favorable transfer efficiency.

The main evaluation parameters in the MCR-WPT systems are self-inductance, mutual inductance, coupling coefficient (k , $0 < k < 1$), Q factor and S-parameters, which all should

be considered in the design process. The self-inductance shows the inductive features of a single coil; it is decided by the coil length, turn and size. The mutual inductance indicates coupling features between two coils [43]. In the WPT system, it indicates how well are the transmitter and receiver sets being coupled. High coupling coefficient means strongly coupled and vice versa. The Q factor characterizes the rate of energy losses of a resonator. The higher the Q factor, the stronger energy storage ability of the resonator. The S-parameters can be used to evaluate the energy delivery performance of a WPT system. S_{11} (input power reflection coefficient, also known as return loss) and S_{21} (forward power transmission coefficient) are of particular interest and are measured in Chapter 4 and 5. These evaluation parameters are being greatly influenced by structural variables such as width, length and turns of the coils, gap between each turn, gap between the resonator and the loop circuit, substrate materials, etc.

There are three charging conditions for the MCR-WPT systems, ‘over coupled’, ‘critically coupled’ and ‘under coupled’ as shown in Figure 2-4, where K_{23} is coupling coefficient between the transmitting and receiving resonators. There is an optimal transmission distance at which the maximum efficiency can be acquired. The ‘critically coupled’ condition occurs at this distance. When the distance becomes smaller than this threshold, the strong coupling between the transmitter and receiver leads to change of inductance and capacitance of system components; the resonant frequency will shift away from the operational frequency and induces the frequency shifting phenomenon [3]. Transfer efficiency thus decreases at the operational frequency; this situation is called ‘over

coupled' which is indicated by the red dashed area in Fig. 2-4. When the distance becomes larger than the optimal distance, the transfer efficiency will drop rapidly due to the aforementioned inverse square relation between the efficiency and distance; this situation is known as 'under coupled'.

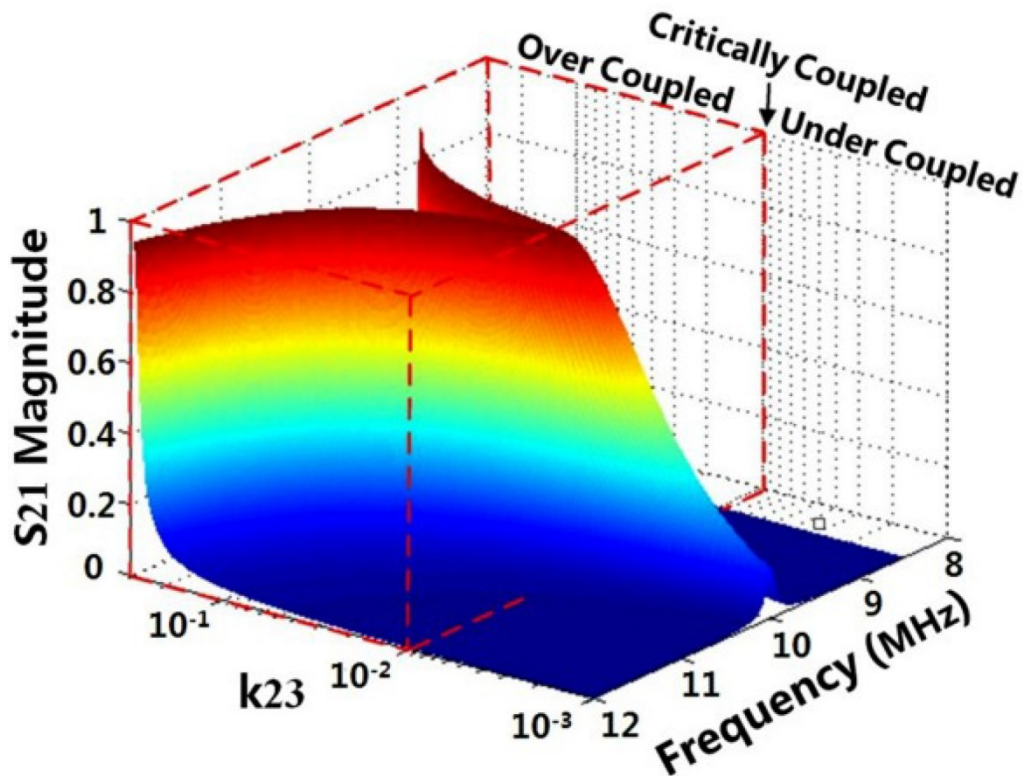


Figure 2-4: Three conditions of MCR-WPT technique [7]

The above-mentioned frequency splitting phenomenon is one of the intensive research topics on MCR-WPT systems. A few methods to overcome this problem have been proposed. For instance, in [3], an adaptive frequency tuning technique has been presented to maintain the maximum transfer efficiency in the over coupled area. In [26], the frequency splitting problem is even worse in the multiple receiver systems because of the strong coupling between receivers when placed in near proximity. A control circuitry was

developed to tackle the situation by tracking the resonant frequency shifts and re-tuning the receiving coil capacitances [26].

The major drawback of the MCR-WPT systems is that the capacitance value for the coils is very sensitive to change of distance, coil parameters, and positions of the charged objects with respect to the transmitter. As the effective methods have been developed, these problems can be well addressed. After all, the MCR-WPT technique is regarded as the best candidate to recharge small electronic devices in this thesis.

2.3 Far-Field Wireless Power Transfer Techniques

Far-field or radiative WPT systems can transfer wireless power over a much longer distance compare to that of the non-radiative systems; they often employ microwaves or lasers can be applied to charge anonymous sensors [44], aerial vehicles and solar power satellites [45]. But the consequent safety issues will need specific attention and standards to regulate their uses, to avoid the exposure of human bodies to hazardous electromagnetic fields.

2.3.1 Microwave Radiation

Figure 2-5 shows a WPT system using microwave radiation; the process can be named microwave power transfer or microwave power transmission. The configuration is similar to that of a wireless telecommunication system; the difference is that the receiver receives energy or power instead of data. The electrical power from the power source, whether it is

DC or AC, is first converted to microwave, sent to the transmitting antenna, propagates into the free space in the form of electromagnetic fields and then intercepted by the receiver. At the receiver, the microwave is converted back to the DC power to charge the load.

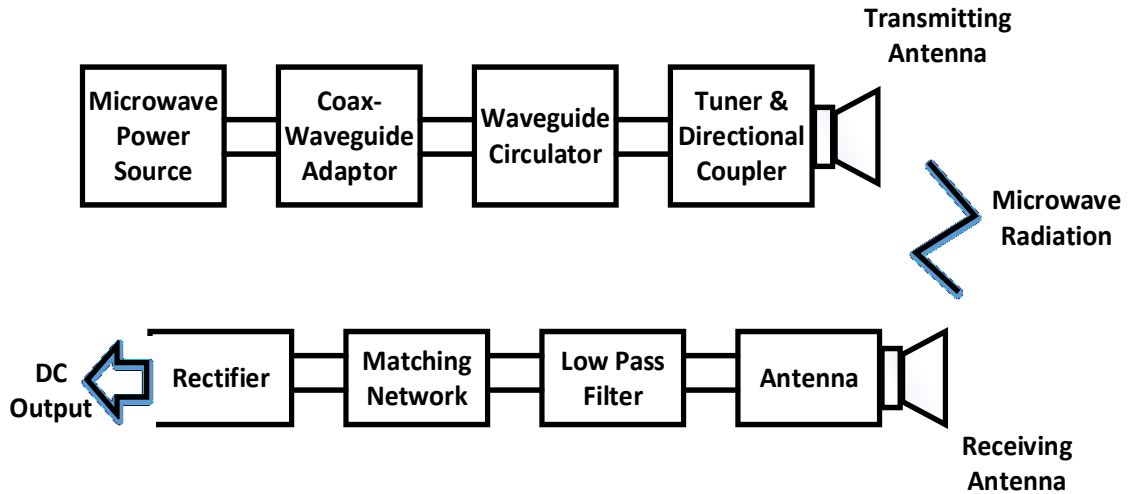


Figure 2-5: Block diagram of microwave power transfer [45]

Kilometers of transmission distance can be achieved using this method, but the key drawbacks are the free space loss and possible high RF density exposure [29] that leads to low power efficiency and safety issues because of its radiation feature. The history, basic theories, features and applications of microwave radiation WPT can be found in [46] and [45].

2.3.2 Laser Beaming

As explained in [29], laser refers to optical amplification based on stimulated emission of radiation. Laser beams are generated from the process as depicted in Figure 2-6. The photons that move from mirror 1 (M_1) to mirror 2 (M_2) along the dashed line direction will

absorb energy when passing through the gain medium, and are transferred from the lower stable state (green arrows) to the upper excited state (curved red arrows). When they arrive at M_2 they are reflected back to M_1 to stimulate more photons (straight red arrows) to repeat the same process. This process creates a very sharp high-power light beam, which is known as a laser beam or resonating beam because its similar to the resonance phenomenon. The laser beaming wireless power transfer system is illustrated in Figure 2-7, where R_1 and R_2 are retroreflectors that filter the photons which are not moving along the perpendicular direction of the retroreflectors. A photovoltaic cell, like a solar panel cell, is installed behind R_2 to convert laser light to electrical energy. The gain medium and R_1 together is called the transmitter, while the combination of R_2 and the photovoltaic cell is the receiver. Hence the energy is wirelessly delivered by the laser beam.

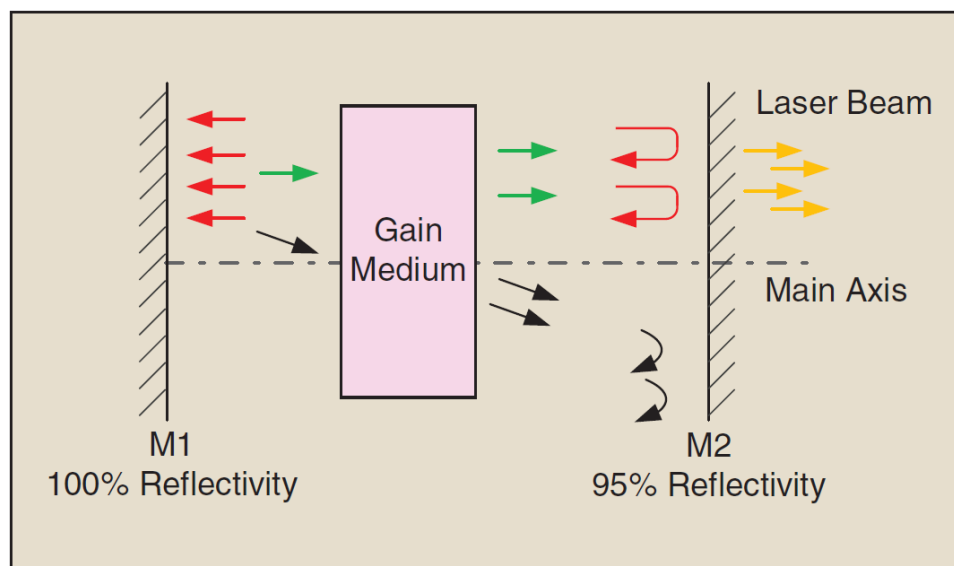


Figure 2-6: The laser fundamentals [29]

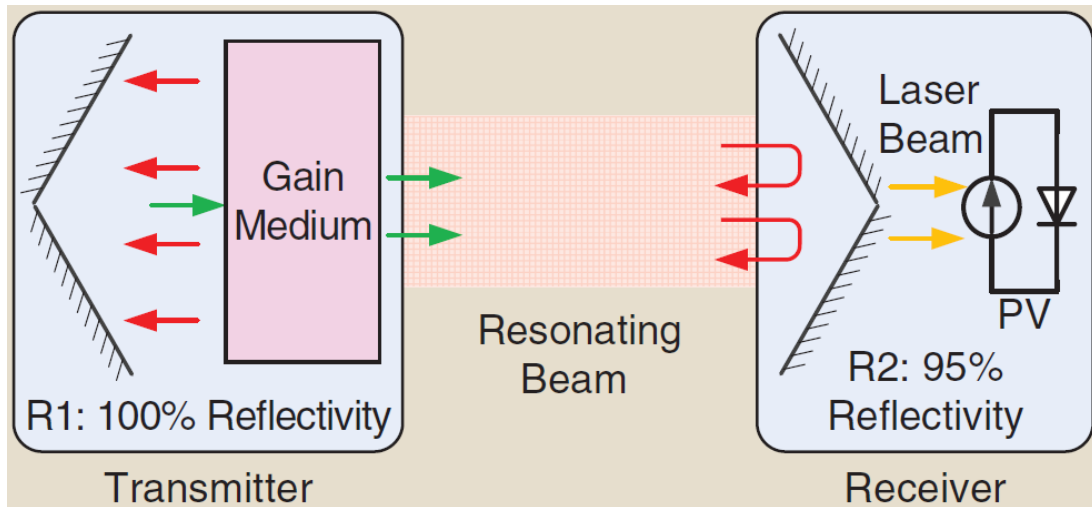


Figure 2-7: Schematic of distributed laser charging [29]

The transmission distance of laser beaming can be extended to several meters. One important requirement for this technique is that the transmitter and receiver must stay within the line of sight since the laser beam can only go cross over transparent objects. This line-of-sight restriction limits the system's mobility to some extent. Another problem is the electromagnetic field exposure of the human body, like microwave radiation. It creates safety issues and requires regulations. The fundamentals, features and applications of the laser beaming method has been concluded in [29].

2.4 WPT for Small Electronic Devices

With all the possible applications described in 2.1.3, the most demanding application is for our daily consumer electronic devices, especially cell phones, which are the target objects in this thesis. The challenges for this specific application and recent research efforts

are presented and discussed in this section.

Generally speaking, only a small space is available for the WPT receivers. In other word, the receivers must be of small size, so they can be attached to portable electronics such as cell phones. The form factors of the receivers have to be small and they make shielding indispensable to avoid internal noises and inductive EM interferences. A handheld MCR charger was introduced in [27] and [47] which suppressed electromagnetic field (EMF) and electromagnetic interference (EMI) noise by using ferrimagnetic material and metallic shielding. Metamaterials were also applied for improvements of WPT systems performance in [48]-[51].

Another matter that needs to be considered for high frequency (MHz or higher) is that power transmission cannot penetrate metallic covers, which effectively separate a transmitter and a receiver. The main cause of the problem is the use of a relatively high frequency, 13.56 MHz, such that skin depth of a metal is much thinner than its thickness. This problem was investigated and solved in [10] by utilizing camera holes in a cell phone that allow magnetic field to pass through. In other words, a proper solution should be developed. One of the other options is to change a metallic cover to a plastic one or glass (like the WPT enabled iPhone 10) to avoid the shielding of the metal phone case.

The size challenge forces the WPT systems designed for small electronic devices must be small enough to become feasible. The laptop model and receiver coils demonstrated in [7] for laptop wireless charging has the dimension of 40 cm³. The receiver presented in [34] is a 32 mm-diameter PCB coil that could be used to recharge small wearable devices.

The receiver coil presented in [8] for cell phone charging has the size of 25×30 mm. One of the trade-offs is that the smaller the size of a receiver, the harder it is to achieve a high transfer efficiency.

Finally, heat generation on metal covers caused by magnetically induced eddy currents is an issue which cannot be ignored [10]. This is normally a problem of inductive coupling that typically operates at a lower frequency range of 100 – 300 KHz. Since the application frequency in this thesis is 13.56 MHz, this will not be a major problem that need to be considered in design.

The solutions to the above issues have been addressed so far to some extent. A wireless charging system for smart phones in Bluetooth environment has been presented in [33]. The system made use of the existing Bluetooth function and charging controller was developed to activate or disable the charging function when Bluetooth is on. The entire system including matching circuit, rectifier and antennas were designed and fabricated with a real commercial film-type integrated board. Since Bluetooth uses microwave, the charging power was only 750 μ A at maximum.

A fabrication process of an aluminum phone cover with complete inductive coupling WPT systems for cell phone recharge has been shown in [10]. A vertical slot from the camera and flash holes to the edges of medal covers and horizontal slots on both broadsides of aluminum covers were created to enable magnetic fields to go through the metal body. A center coil was placed around the camera lens to maximize strongly coupling to the transmitter. Two side coils on both left and right edges were designed and in serial

connection with the central coil as a complement to intensify mutual coupling. The mutual inductance between the medal cover and the receiving coil embedded in a cell phone was optimized based on the induced voltage. Ferrite structures were combined into the system to confine magnetic fields. They were placed to cover the center coil with two major roles: one is to magnetically shield the coils from nearby metallic objects and another is to increase self-inductance of the coil and in turn enhance mutual inductance between the transmitter and receiver.

An aluminum body of a cell phone with enabled wireless charging function at 6.78 MHz was fabricated with a circuit card that integrates impedance matching network, rectifier, EMI filter, converter and shielding [10]. The central receiving coil attached to the aluminum body had the size of 25mm×30mm with the coil diameter of 0.25mm and the space of 0.5mm between two consecutive turns. The entire system including the coils and the circuit integrated with the aluminum case whose volume was comparable to that of a typical handset, 136 × 70 × 8 mm. The aluminum thickness was 1mm. The power transfer efficiency between the certified AirFuel Alliance transmitter and the receiver was measured to be 90%. The measured load power ranged from 6.8 W to 8.2 W which is suitable for mobile devices. The rectified voltage, current as well as the temperature of the aluminum cover were also tested. Besides, how the camera openings and slots on the aluminum sheet as well as ferrites affect inductance, resistance and mutual coupling were experimentally investigated. Simultaneous wireless charging of three aluminum encased phones placed on the same transmitter were also tested; the results showed the multi-

receiver charging capability of the proposed system [10].

The system proposed in [10] has the highest transfer efficiency reported to date for wireless cell phone charging, and the entire system was fabricated and proved to be practical by measurements of output power and charging three of Samsung mobile phones in one charging pad. However, it requires sophisticated multistage manufacturing process that raises cost and difficulty in producing it in a large quantity. Also, it provides very limited spatial freedom since the mobile phones had to be physically in contact with the transmitter to achieve maximum power transfer efficiency.

A controlled resonance technology was proposed in [28] for charging mobile phones with relatively good spatial freedom. The entire system consists of a magnetic shield, receiving and transmitting coil windings, and a metal back cover between them. The technical keys are the bipolar windings of the transmitter and receiver as well as the hole in the middle of the metal back. The opening has the same function as that presented in [10] for magnetic fields to pass through the metal. Another advantage with this opening design was that the hole together with the bipolar windings enabled the enhancement of the magnetic coupling by the eddy current in the metal around the opening [28]. A 70% system efficiency was achieved with a 10 W power available at the load.

2.5 Auxiliary Materials

Magnetic materials are known to be capable of confining and leading magnetic flux because they possess high relative permeabilities. They can be used to improve self-

inductances of coils and coupling between them. The ferrimagnetic material is one of the popular magnetic materials and is widely used to confine and guide magnetic flux because of its high relative permeability (e.g., $\mu_r > 1000$) and low conductivity (e.g., $\sigma < 10^2 S/m$). These properties are beneficial to the WPT systems and lead to improved performances.

Ferrites have been used in [16] to increase magnetic fluxes and coupling in helices for small devices. The analytical relationship between the Q factor of the helices and their geometrical parameters with ferrite cores were given in [16], and the expression of Q factor can be used to derive the maximum power transfer efficiency of a helix with a ferrite cylinder core.

The problem that electromagnetic field emission is potentially harmful to the surrounding living organisms was pointed out in [17]; thus, magnetic emission should be minimized using shields without compromising system performances. Shields can be divided into passive and active ones. With passive shielding, magnetic field is reduced by a combination of blocking of low resistivity metals like aluminum and low magnetic resistance materials such as ferrites. Active shielding is developed by having additional fields in opposite directions to the fields surrounding the primary coil. Active shielding was used in [17] with secondary coil to generate an opposite magnetic flux to reduce the overall magnetic fields.

An MCR-WPT system topology for electrical vehicles was proposed in [17] with the litz coil embedded in a ferrite disc. A similar structure can be found in [18] for 100W-class

WPT system. The magnetic coupling coils were surrounded by ferrite materials as well. The difference between [17] and [18] is that the aluminum shield is incorporated with the ferrite material by surrounding it. The comparisons between different systems with different shielding materials were made in [18]; they showed that the magnetic fields were greatly confined and had significantly less leakage with the improvement of system performance.

The common issue of the ferrite structures described in [17] and [18] is that the complex ferrite structures are hard to produce in numbers and to maintain with ferrite fragility.

The ferrite structures used for planar WPT systems can be found in [19, 20, 45]. The problem for cell phone WPT applications is that when the receiver is positioned close to the adjacent conductive objects such as a battery and a metal case, the Q factor of the receiving resonator is degraded [40]. In [19], four receiver structures were proposed and compared. They include a receiver coil, a receiver coil on a conductor, a receiver coil with ferrite sheet and conductor, and a receiver coil with two-layer ferrite sheet and conductor. The results showed that the receiver coil with single-layer ferrite sheet and conductor has the highest relative permeability and the lowest loss. The reason why the two-layer ferrite structure lead to a worse scenario was because of the losses caused by the ferrites. An air gap was added in [20] between the ferrite sheet and metal strip. The magnetic flux distribution and magnetic shielding results demonstrated the air gap between the ferrite plate and metal strip is effective for the shielding performance as well as the power transfer efficiency. The reason is because the eddy current cancellation has been decreased with the

air gap [20]. A novel ferrite shield with an auxiliary loop on a ferrite in a metallic environment was proposed in [52]. After comparing with the traditional topology, 30% transfer efficiency was achieved due to the auxiliary loop on the ferrite.

When the ferrite sheet is introduced into the WPT systems, different coil winding methods can influence the effects of ferrites as well. This problem has been investigated in [23] with different coil topologies for inductive power transfer. The results showed that when ferrites are used, the single square coil structure is the most suitable candidate to achieve the good system performance.

As mentioned before, The disadvantages of the ferrites are the eddy current losses in high frequencies and hysteresis losses; the details can be found in [18] and [52].

2.6 WPT Using MCR for Small Electronic Devices

Based on the discussions presented above, the MCR technique is chosen as the most suitable method for recharging small consumer electronics. The following sections review and summarize the MCR-WPT systems.

2.6.1 Coil Structures

Most MCR-WPT systems proposed in the literature are of three-dimensional, such as helical coils presented in [42]. The disadvantages of the three-dimensional structures are that the coils are bulky in geometry and precise fabrication is necessary to maintain a high Q-factor, making them less feasible or even impossible for small mobile devices and

implanted medical devices.

In order to make the WPT system small and more applicable, efforts have been made in [8] to use the planar coil rings or spiral coils instead of helical coils. The size of the WPT systems were decreased by reducing the distance between the resonators and the source or load loops. In the planar structures, the gap between the transmitter resonator and the source loop is reduced to zero and so is the gap between the receiver resonator and the load loop. In [3], four coils were being laid on two planes. The helix, spiral coil and coil ring geometries for resonant WPT were compared in [53]. In recent years, the printed spiral coils (PSCs) were developed and became popular in both research community and industry [11]-[15]. The transmitter and receiver coil sets were fully planarized and printed on one side of RF4 substrates, making the system even thinner and practical for applications. These fully-planar MCR-WPT systems have the advantages of low profile, small footprint and easy fabrications when compared to three-dimensional coils; they make the systems much portable and feasible to be attached to or implemented in small electronic devices [11].

The symmetric, planar MCR-WPT systems designed for small electronic devices have been described in [12] and [11], and achieved the highest efficiency of 74.1% and 82.8%. The coil configurations were optimized for the transmitter and receiver, and they realized the optimum power transfer at the distance of 20 cm and 10 cm respectively. Additionally, asymmetric transmitter and receiver designs can be found in [3, 10], with a receiver size smaller than the transmitter size. This asymmetric configuration can better solve the trade-

off problem between power transfer efficiency and system mobility than the symmetric one. It also mitigates axial and angular misalignment problems. Nearly 80% transfer efficiency was achieved by the asymmetric, planar MCR-WPT system with the distance of 7 cm [41]. The transmitter and receiver sizes were 200 mm² and 100 mm² respectively.

The three-dimensional L-shape configuration was proposed in [14]. The size of transmitting and receiving resonators were 62×33×5 cm. The 84.38% power transfer efficiency was obtained with the transmitter and receiver sizes of 100×100×1.6 mm and 70×70×0.8 mm, respectively. The lateral misalignment problem has been greatly improved by the L-shape topology, validated through electromagnetic fields distributions. An intermediate coil was placed in between the transmitter and receiver in [7], acting as a “repeater” to extend the WPT distance. An intermediate self-resonator was also designed in [21] and placed perpendicularly between the transmitting and receiving resonators to constitute a “ π ” shape configuration. The comparison between the coaxial and perpendicular arrangements of the intermediate resonators [21] was made with the conclusion that the efficiency of an MCR-WPT system with the primary resonators and the intermediate resonator arranged perpendicularly is as good as that of a coaxially arranged system within a certain area. An asymmetric MCR-WPT system with around 80% power transfer efficiency within 100 cm transmission distance was validated as well in [21].

2.6.2 Coil Shapes

Square [11]-[13] and circular [3, 6, 25] coils are two commonly used basic geometries for WPT systems. The mutual inductance is the key figure in magnetically coupled systems, since it determines quantity of magnetic flux that goes through receiver coils and thus decides power transfer efficiency [4]. The comparison between circular and square coils were done in [4] which shows that the square coil has larger inductive area than the circular coil does when the dimensions (diameter of circle and length of square) are the same. The drawback is that magnetic flux distribution of square coils is not cylindrically symmetric, resulting in higher calculation time and larger memory space. Because their flux distribution is mirror symmetric at least, square coils are more acceptable and popular than the circular ones.

The analytic and measurement results showed that the circular and square coil have similar S-shapes (climb - surge - climb) of self and mutual inductance [4]. This finding indicates that when high permeability materials such as ferrites are used, better power transfer efficiency will be achieved. Another interesting finding of [4] is that the self-inductance increases faster than the mutual inductance; it means the coupling coefficient will decrease with increasing permeability [4]. This is caused by the energy losses of the high permeability materials.

2.6.3 Planar MCR-WPT for 13.56 MHz Applications

The planar MCR-WPT for charging small electronic devices at 13.56 MHz is selected

to achieve WPT in this thesis. This frequency is licensed for RFID applications that form an important part of Internet of Things (IoT). The recent WPT work on these applications can be found in [11]-[13]. The novel MCR-WPT systems being proposed in Chapter 4 of this thesis are the continuity of the published work. Their comparisons and improvements will be demonstrated in Chapter 4 and Chapter 5.

A planar wireless power transfer system through strongly coupled magnetic resonance was proposed in [12]. Both the transmitter coil set and the receiver coil set were fully planar and printed on one side of a FR4 substrate with the size of 200 mm² and thickness of 1.6mm. Both the transmitter and receiver units have lumped capacitors connected. At the operating frequency of 13.56 MHz, a maximum transfer efficiency of 74.1% can be achieved at the distance of 200mm between transmitter and receiver.

Effects of ferrimagnetic materials and perfect electric conductors were also investigated. At the distance of 200 mm, two rectangular ferrite sheets were firstly placed behind the transmitter and receiver sets respectively and then replaced with the copper plate of the same thickness. The maximum power transfer efficiency of the system is increased from 76% to 82.8% in the presence of ferrite plates, whereas it is reduced by 71% with the copper plates.

The optimization process of the WPT system in [12] has been demonstrated in [11] with the geometric parameters provided. The equivalent circuit model of the proposed system was analyzed first. The analytical expressions of resistance R, inductance L and capacitance C for each coil circuit were found through mathematical calculations. Then,

the matrix equation for the relationship among current I , voltage V , impedance Z and mutual coupling coefficient M are given. An optimization algorithm for dimensional parameters was developed to produce the optimum transfer efficiency, and explanations were given on how each variable affects the system performance. In addition, the phenomenon of frequency splitting and how the input impedance affect the transfer efficiency were investigated.

It was shown that increase of the space between two spiral coils will result in the decrease of Q factor. To compensate for the decrease, auxiliary strips were added and utilized in [12] without changing the low profile of the planar WPT system. Two identical auxiliary strips were applied first to the backside of transmitter and receiver, respectively, and are connected to the primary resonators on the opposite sides of the substrates through via. The measured transfer efficiency was increased from 77.27% to 79.75%, and further increased by 82.67% through adding the shorting walls that conductively connected the primary coil and auxiliary coil. Without the shorting walls, a second auxiliary strip can be added. By putting the two boards together, a three-layer resonator that has three repetitions of the resonating coils was reported to improve the transfer efficiency from 79.75% to 82.01%. By adding shorting wall to the three-layer resonator, a further maximized efficiency of 84.38% was achieved.

2.7 Summary

The configuration, classifications, applications and challenges of the WPT systems are

discussed in this chapter. The focus in this thesis is to develop an MCR-WPT system that suitable for small electronic devices. With a large amount of existed WPT systems and results reviewed in this chapter, there are always defects that prevent the better application for small electronic devices. The challenges face the WPT systems for small electronic devices require WPT designers to design novel WPT systems that are implantable or attachable to small mobile devices specially cell phones with good system performance. Moreover, good free-positioning capability and misalignment performance are desirable to be standout from the existing systems.

CHAPTER 3 OUR DESIGN METHODOLOGY

The methods used in our designs are discussed in this chapter. The equivalent circuit of the ferrite-less structure is given at first with mathematical formulas provided for circuit parameters including transfer efficiency. Incorporation of ferrite materials into the WPT systems to improve system performance is then described. The analytical solutions of the ferrite incorporated systems are not available due to non-linearity of ferrite properties. Therefore, electromagnetic simulators, ANSYS High Frequency Structure Simulator (HFSS) is used to compute ferrite structures. The simulator uses a numerical method called Finite Element Method which will also be briefly introduced.

3.1 Theoretical Analysis

The planar MCR-WPT system was built first and then incorporated with the ferrite structures. The equivalent circuit model for a conventional four-coil planar MCR-WPT system without ferrite is shown in Figure 3-1. The 'M' represents mutual coupling: for example, M_{12} is the mutual coupling between the source loop and transmitting resonator, while M_{14} is the mutual coupling between the source loop and the load loop. In order to get the transfer efficiency, the key point is to figure out mutual coupling coefficients [11].

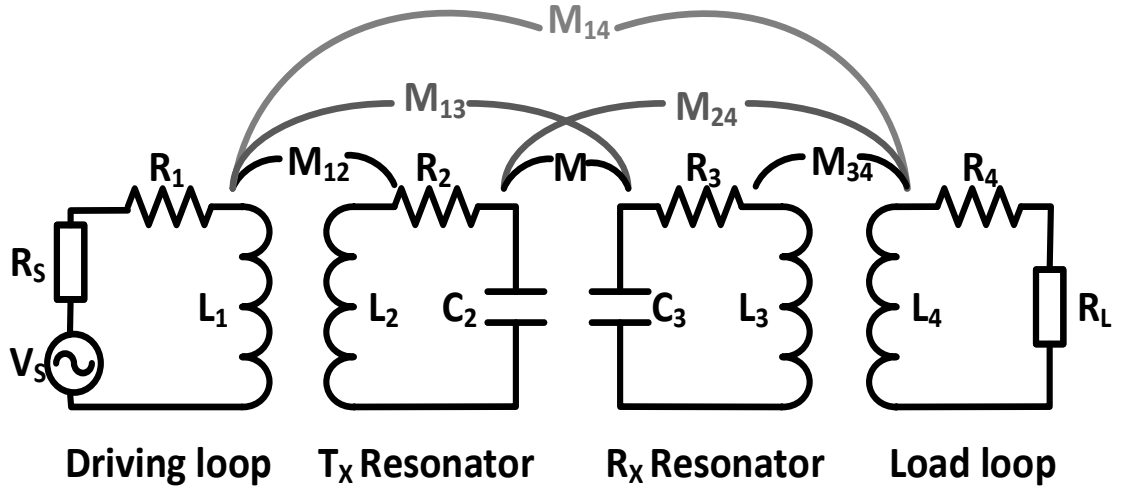


Figure 3-1: Equivalent circuit model of the planarized MCR-WPT system

As presented in [11], the key circuit parameters including inductance, capacitance and resistance for each loop and resonator can be expressed as (3-1), (3-4) and (3-6). Printed spiral coils were considered in this thesis.

The expression for the self-inductance of the PSCs is:

$$L = \frac{1.27 \mu_0 n^2 r_{avg}}{2} \left[\ln \left(\frac{2.07}{\varphi} \right) + 0.18\varphi + 0.13\varphi^2 \right], \quad (3-1)$$

where μ_0 is the permeability in free space, n is the number of PSC turns, r_0 and r_i are the outer and inner radii of the coil, and

$$r_{avg} = \frac{(r_0 + r_i)}{2}, \quad (3-2)$$

$$\varphi = \frac{(r_0 - r_i)}{(r_0 + r_i)}, \quad (3-3)$$

where φ is the fill factor.

The capacitance can be calculated as:

$$C = (0.9\varepsilon_{air} + 0.1\varepsilon_{sub})\varepsilon_0 \frac{t}{s} l_g, \quad (3-4)$$

$$l_g = 4(2r_0 - W_r \cdot n)(n-1) - 4s \cdot n(n+1), \quad (3-5)$$

where l_g is the length of the gap, W_r is the width of the resonator coil and s is the gap between two turns of resonator coil as depicted in [41] (figure 4-1). ε_{air} and ε_{sub} are the permittivity of air and the substrate respectively.

The resistance of a PSC can be expressed as:

$$R_S = R_{skin} + R_p. \quad (3-6)$$

The resistance is the sum of the resistance due to skin effect and the resistance due to proximity effect. They can be expressed as follows:

$$R_{skin} = R_{dc} \left(\frac{t}{\delta \left(1 - e^{-\frac{t}{\delta}} \right) \left(1 + \frac{t}{W_r} \right)} \right), \quad (3-7)$$

where R_{dc} is the DC resistance, δ is the skin depth and t is the thickness of the conductive trace.

$$R_p = R_{dc} (\beta f + \sigma f^2), \quad (3-8)$$

where f is the frequency, β and σ are fitting coefficients to be determined

empirically [11].

Mutual inductance M can be calculated using equation (3-9). Since the distance between each loop and resonator is relatively large for the conventional three-dimensional MCR-WPT systems, only the mutual inductance between the proximal coils is taken in to account (i.e., M_{12} , M and M_{34}). A modified equation to calculate M for planar MCR-WPT systems was used in [11]. The M_{12} , M_{24} and M_{14} cannot be omitted in this case because the loop and resonator are printed in the same substrate and close to each other; thus, a more precise equation for mutual inductance is given in [11] as

$$M = \left(\frac{4}{\pi}\right)^2 \sum_{i=1}^{i=n_1} \sum_{j=1}^{j=n_2} M_{ij} \quad (3-9)$$

and

$$M_{ij} = \frac{\mu_0 \pi a_i^2 b_j^2}{2(a_i^2 + b_j^2 + z^2)^{\frac{3}{2}}} \left(1 + \frac{15}{32} \gamma_{ij}^2 + \frac{315}{1024} \gamma_{ij}^4 + \frac{15015}{65536} \gamma_{ij}^6 + \dots + 0.6028 \gamma_{ij}^{28} \right), \quad (3-10)$$

where a_i and b_j are defined in [11] and error of this formula was reported as 0.52%.

Now the matrix equation based on Kirchoff voltage law for the four-port network in Figure 3-1 can be written as:

$$\begin{bmatrix} I_2 \\ I_2 \\ I_3 \\ I_4 \end{bmatrix} = \begin{bmatrix} Z_{11} & (j\omega M_{12}) & (j\omega M_{13}) & (j\omega M_{14}) \\ (j\omega M_{12}) & Z_{22} & (j\omega M) & (j\omega M_{24}) \\ (j\omega M_{13}) & (j\omega M) & Z_{33} & (j\omega M_{34}) \\ (j\omega M_{14}) & (j\omega M_{24}) & (j\omega M_{34}) & Z_{44} \end{bmatrix}^{-1} \begin{bmatrix} V_s \\ 0 \\ 0 \\ 0 \end{bmatrix}, \quad (3-11)$$

$$Z_{11} = \left(R_s + R_1 + j\omega L_1 + \frac{1}{j\omega C_1} \right), \quad (3-12)$$

$$Z_{22} = \left(R_2 + j\omega L_2 + \frac{1}{j\omega C_2} \right), \quad (3-13)$$

$$Z_{33} = \left(R_3 + j\omega L_3 + \frac{1}{j\omega C_3} \right), \quad (3-14)$$

$$Z_{44} = \left(R_4 + R_L + j\omega L_4 + \frac{1}{j\omega C_4} \right), \quad (3-15)$$

where C_1 and C_4 are the parasitic capacitances of the driving loop and the load loop, respectively. The transfer efficiency can be acquired by solving the above matrix equation. The ratio between the voltage obtained at the load and the source voltage (V_{load}/V_{source}) can be calculated first and the expression of transfer efficiency is then:

$$\eta = |S_{21}|^2 = \frac{V_{load}^2 / R_{load}}{V_{source}^2 / (4R_{source})}. \quad (3-16)$$

The capacitor-loaded PSCs structure is used to achieve MCR-WPT. It can be regarded as an equivalent RLC resonating circuit. The capacitor can be used to adjust resonant frequencies based on the relationship among frequency, inductance and capacitance (3-17):

$$f_r = \frac{1}{2\pi\sqrt{LC}}. \quad (3-17)$$

The optimization scheme based on the above mathematical analysis and theoretical results was proposed in [11].

3.2 Ferrite Materials

As mentioned in section 2.5, ferrite structures can be used to confine magnetic field,

resulting in larger inductance. One of the reasons is that ferrite materials have high relative permeability (usually greater than 1000 H/m) and low conductivity (mostly less than 102 S/m). This characteristic can improve mutual inductance and self-inductances of the coupled coils as well as reduce magnetic field leakage around the source. More specifically, ferrite materials can play the following three roles: confine magnetic field, mitigate magnetic leakage and shield magnetic interference.

However, ferrite structures have their downsides too. They are normally very fragile; it makes difficult to attach them to anything. Moreover, ferrite structures are hard to produce in numbers with inconsistent electrical properties. Finally, eddy current loss and hysteresis losses become significant at high frequencies (MHz or higher) [2]. For instance, the double-layer ferrite system presented a worse power transfer efficiency than the single layer system because of the losses [3].

Considering the pros and cons of various ferrite structures and functions, this thesis presents and studies the three ferrite structures: ferrite core, ferrite plate and ferrite sheet, for implementations with the planar MCR-WPT systems for small consumer electronics. They are incorporated to develop the new symmetric and asymmetric WPT systems with improved power transfer efficiency and reduced impact by metal objects. The design specifications and improvement results will be discussed in Chapters 4 and 5.

3.3 The Finite Element Method

Because of the nonlinear behaviors of ferrites, analytical solutions to ferrite structures

are not available. Numerical methods have to be applied for theoretical analysis of the structures. To this end, the well-known High Frequency Structure Simulator (HFSS) by ANSYS is used in this work. It is powerful in computing electromagnetic field distribution and scattering parameters [54]. It uses the Finite Element Method to find solutions of Maxwell's equations.

The way HFSS works is that a solution domain is subdivided into numerous small elements (e.g. tetrahedrons) first. The field solution within each element is expanded in terms of a preselected shape function. Maxwell's equations are then applied, and the expansion coefficients are found in an approximate manner. Once the coefficients are found, an approximation to Maxwell's equations is then found. Because tetrahedrons can be used to approximate any arbitrary three-dimensional geometry, the HFSS is able to solve any problem with complex shapes of spatial boundaries or interfaces.

In this work, the HFSS is used to compute the S parameters of the proposed systems and magnetic characteristics by plotting electromagnetic field distributions. The optimization process is finished by optimizing the variables in the system geometries to have the best power transfer efficiencies.

3.4 Summary

In our design and optimization approaches, the conventional ferrite-less systems are studied first to understand how each geometric variable influence system performances. Then, different ferrite components are investigated and incorporated into the WPT systems

with HFSS. Finally, the optimized structures are fabricated and measured. Comparisons are made to verify the design results.

CHAPTER 4 THE PLANAR SYMMETRIC MCR-WPT SYSTEM

The objective of this chapter is to design a planar MCR-WPT system with size constraint of 32 mm². The ferrite-less system is given first, and the relationships between system geometric parameters and system evaluation parameters are discussed and used to optimize design in section 4.1. The geometric parameters include the width of and the gap between the copper coils, and system evaluation parameters refer to self-inductance, mutual inductance and quality factor. The ferrites then being integrated into the ferrite-less system to improve system performance. The optimized transmitter and receiver are fabricated, and measurement results are presented as well. Comparisons between simulation and measurement results were made and are described in the results section of this chapter.

4.1 Design

4.1.1 Design Parameters Selections

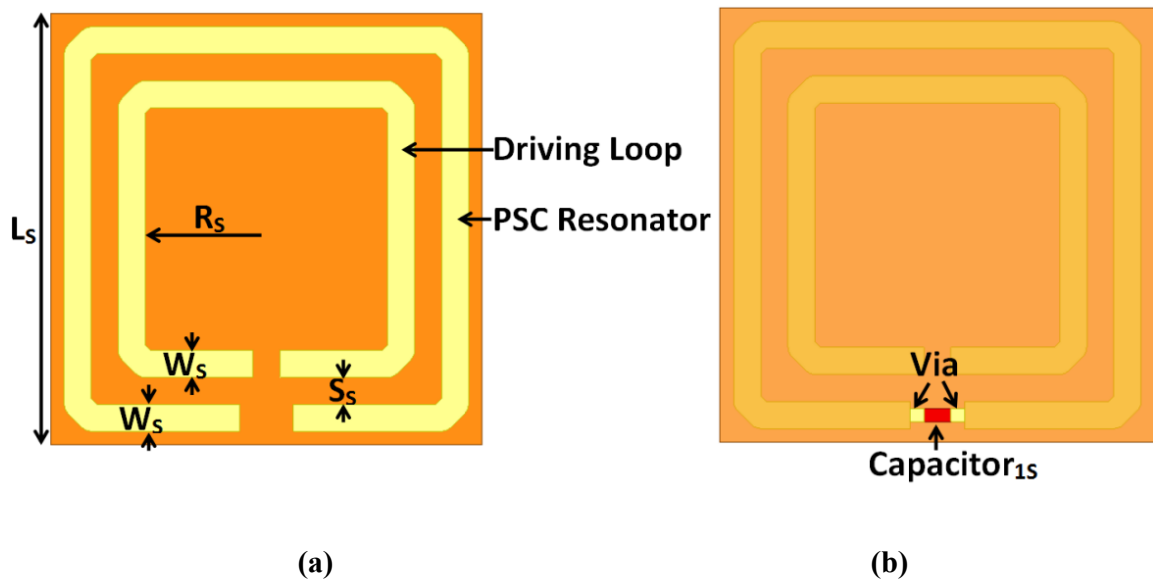
As mentioned before, the square-shaped coil structure is chosen for our development. The main advantage is that when ferrites are incorporated, the rectangular coil has better power transfer efficiency performance than their circular counterpart.

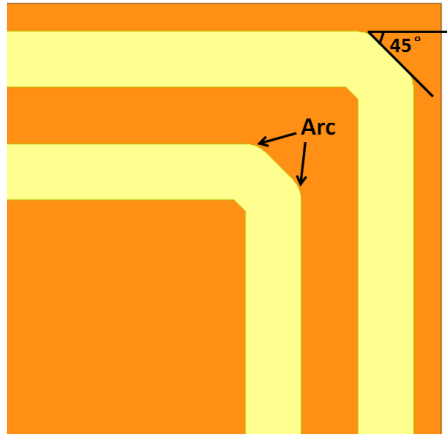
The key performance parameter of the proposed system is power transfer efficiency as it is affected by coil widths, turns, and the gaps between the loop and resonators. It was

shown in [11] that the wider and more turns of the resonating coils, the higher self-inductance, Q factor and power transfer efficiency. However, because of the size limit, the gap between each turn has to be small. Consequently, parasitic capacitances significantly arise, resulting in impedance mismatch. The number of turns of resonant coils has been optimized to be one turn using the optimization scheme proposed in [11] under the 32 mm size constraint. The gap between the loop and resonator is then fine-tuned with HFSS to achieve the maximum power transfer.

The optimized symmetric planar MCR-WPT system receiver without ferrite is shown in Figure 4-1. The dimensional parameters as well as capacitor value are listed in Table 4-

1.

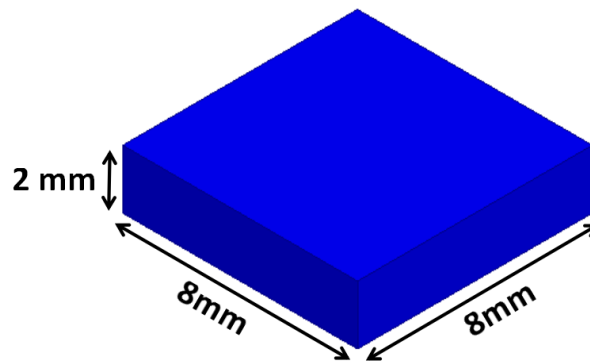




(c)

Figure 4-1: The proposed ferrite-less symmetric WPT system transmitter and receiver; (a) front view, (b) back view and (c) view of the corner.

A ferrite cubic core (which can confine magnetic fields) and a ferrite plate (which can both confine and mitigate magnetic leakage) are incorporated into the symmetric ferrite-less WPT system to improve the system performance as depicted in Figure 4-2. The dimensions of the ferrite core and the ferrite plate are $8 \times 8 \times 2$ mm and $26.42 \times 26.42 \times 1.91$ mm respectively.



(a)

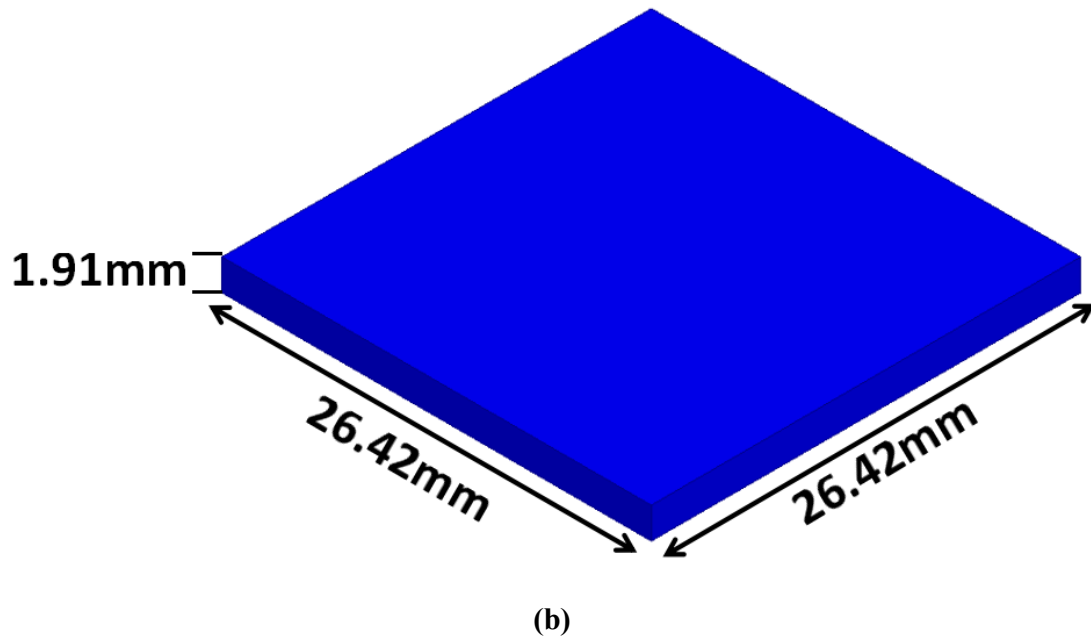
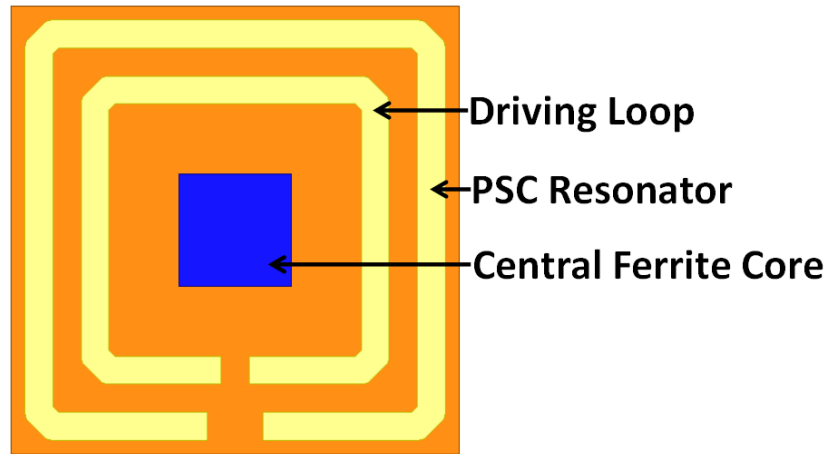
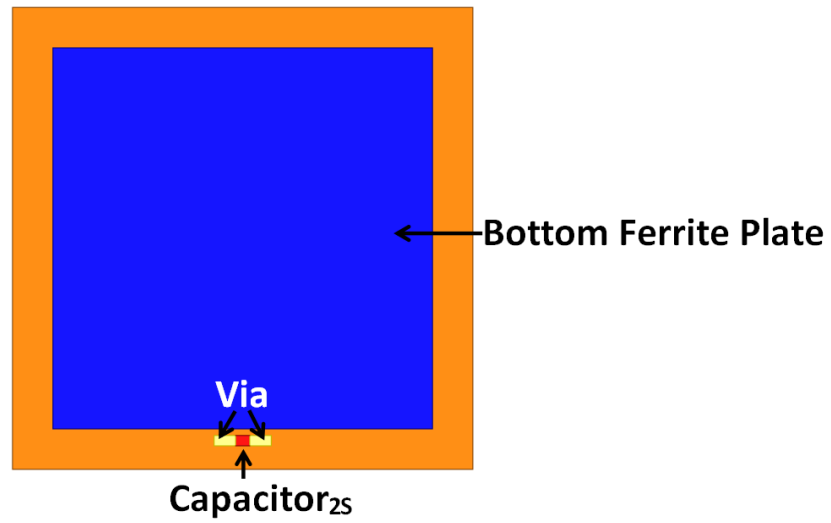


Figure 4-2: The Ferrite structures being used for the proposed symmetric MCR-WPT system; (a) central ferrite core, (b) bottom ferrite plate.

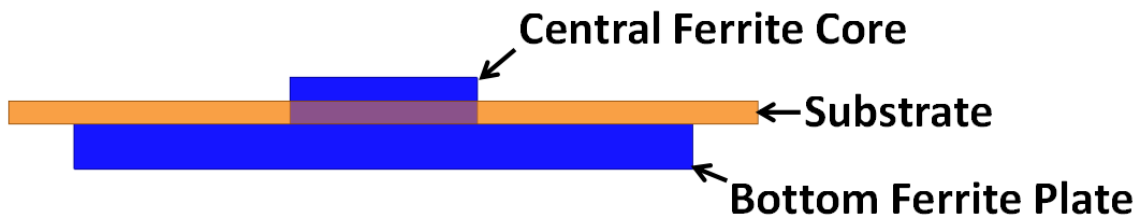
The receiver of the ferrite incorporated system is shown in Figure 4-3. It has a hole of $8 \times 8 \times 1$ mm in the middle of the substrate which the ferrite core places in, while the upper half of the ferrite core emerges above the substrate like a bump as seen in the side view in Figure 4-3. The capacitor values are equal to 1.8 nF for the ferrite-less system and 2 nF for the ferrite incorporated system; they satisfy equation (3-17) when f_r equal to 13.56 MHz.



(a)



(b)



(c)

Figure 4-3: Structure of the proposed symmetric WPT system transmitter and receiver with ferrites; (a) front view, (b) back view, (c) side view.

Table 4-1: Design parameters for symmetric MCR-WPT system

| | | | |
|------------------------------------|------------|------------------------------------|-------------------------|
| L_s (mm) | 32 | R_s (mm) | 9 |
| W_s (mm) | 2 | Central Ferrite Core (mm) | 8×8×2 |
| S_s (mm) | 2 | Bottom Ferrite Plate (mm) | 26.42×26.42×1.91 |
| Capacitor_{1s} (nF) | 1.8 | Capacitor_{2s} (nF) | 2 |

The bottom ferrite plate is chosen because it possesses the closest size to that of the substrate available from the manufacturer. The central ferrite of different sizes are simulated and the $|S_{21}|$ results are shown in Figure 4-4. A slight improvement can be observed with the increase of the length of cubic ferrite core (from 8 mm to 11mm and 15 mm) while the height remains 2 mm. The frequency shifts occur due to changes of system configurations that affect system inductances. Since larger ferrites are more expensive and more fragile, the smaller one is preferred to the larger one because improvement of the power transfer efficiency is not significant with the increase of the sizes.

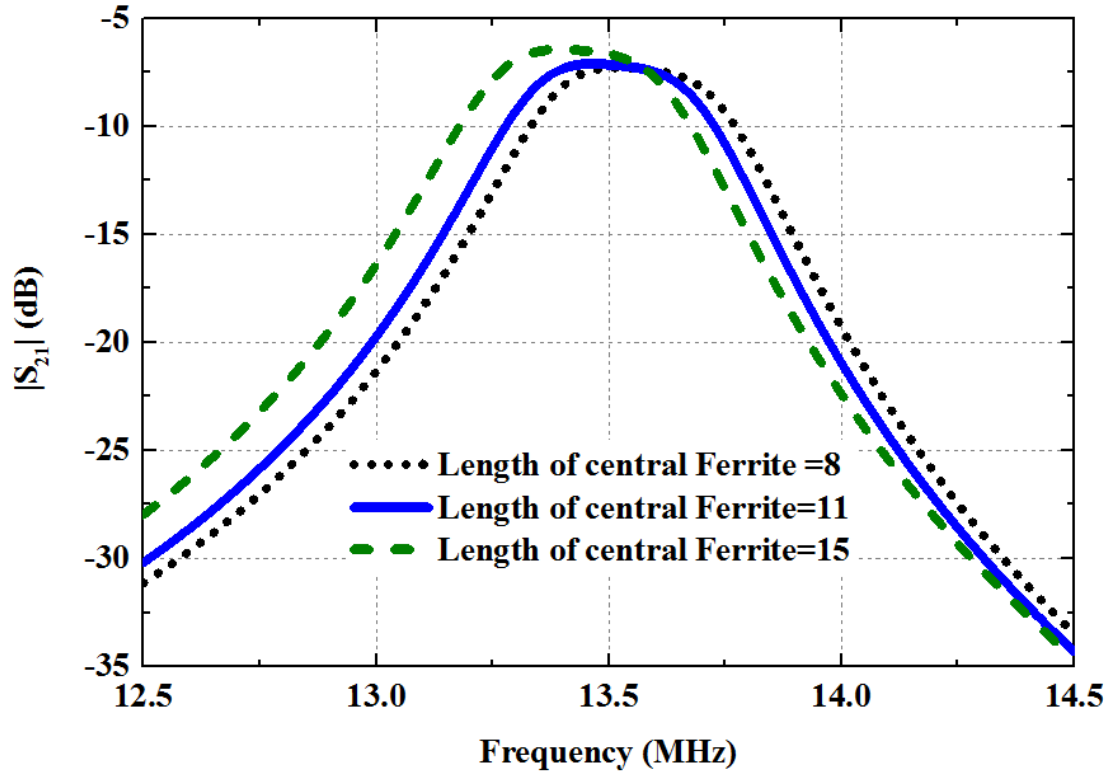


Figure 4-4: S_{21} versus sizes of central ferrite with the symmetric WPT system

4.1.2 The Proposed System

Because of the reciprocity, the proposed receiver structures can also be used as the WPT transmitters for our testing purpose. The optimized system with the ferrite structures is shown in Figure 4-5, where d is the transfer distance between the transmitter and the receiver.

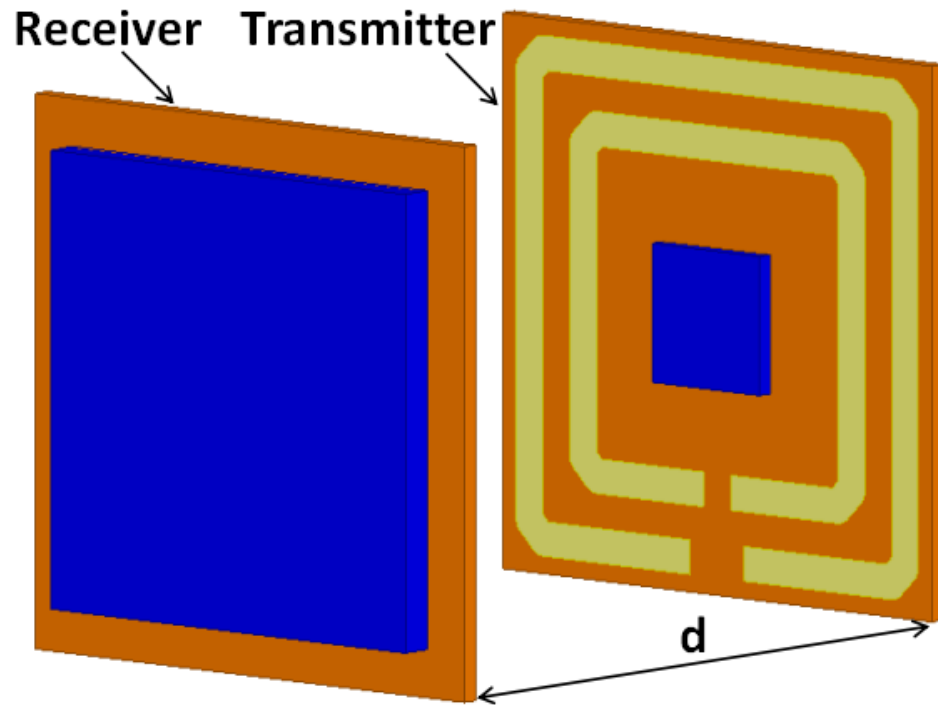


Figure 4-5: Overview of the proposed symmetric WPT system

4.2 Results

The symmetric MCR-WPT systems proposed in section 4.1 are then fabricated and the test is set up as seen in Figure 4-6 and Figure 4-7. The receiver and transmitter components are smaller than half of an iPhone 6s as shown in Figure 4-8.



Figure 4-6: The conventional WPT system and its test setup.



Figure 4-7: The proposed system with the ferrite structures and its test setup.



Figure 4-8: The conventional and the proposed WPT receivers in size comparison of iPhone 6s.

From the simulated and measured results, the distance of 35 mm between the transmitter and the receiver is the optimized transmission distance for both the conventional MCR-WPT system and the proposed system with the ferrites at the operational frequency of 13.56 MHz. The comparisons of S_{21} parameter between the conventional system and the proposed system with or without ferrites are listed in Table 4-

2. The results show that the central ferrite core can improve the transfer efficiency $|S_{21}|$ by 0.5 dB, while the incorporation of both the central ferrite core and bottom ferrite improve the transfer efficiency $|S_{21}|$ by 3 dB. The simulated maximum transfer efficiency is improved from 16.6% to 33.1% after the ferrites are incorporated.

Table 4-2: The simulated results of S_{21} parameter with or without ferrites

| $ S_{21} $ (dB) | With Bottom Ferrite Plate | |
|---------------------------|---------------------------|------|
| | Yes | No |
| With Central Ferrite Core | | |
| Yes | -4.8 | -7.3 |
| No | -5.3 | -7.8 |

Measured transfer efficiencies are also compared with those of the simulated results as shown in Figure 4-9. A big difference between the transfer efficiencies of the conventional WPT system without ferrites and the proposed system with ferrites is shown. They verify the effectiveness of the ferrite materials in improving the WPT system performances. The peak values of the efficiency are 33.1% by simulation and 32.8% by measurements. The simulation and measurement results are in good agreement. The slight differences between simulation and measurement results are due to fabrication errors as well as non-ideal printed circuit boards and capacitors used.

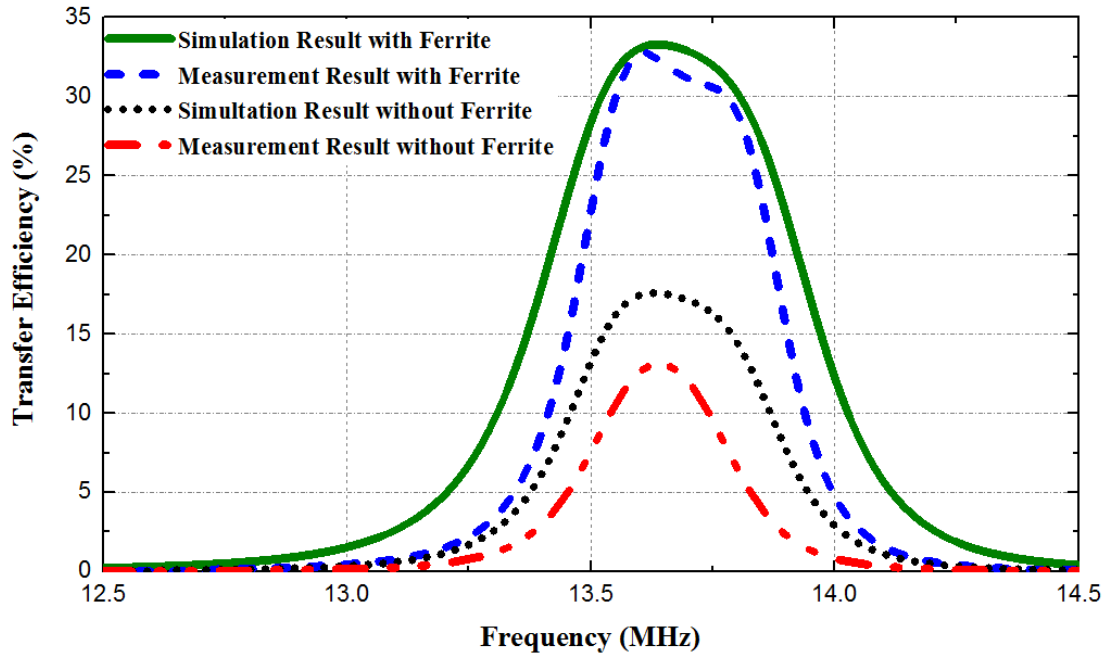


Figure 4-9: Measured and simulated transfer efficiency of the symmetric WPT system with or without ferrite with 35 mm air gap.

For the proposed system with ferrites, the power transfer efficiencies are measured at every 10 mm step from 10 mm to 80 mm of the distance between the transmitter and receiver. The results are shown in Figure 4-10. The frequency splitting phenomenon is observed in the first three curves when the transmission distance is smaller than 30 mm. When the distance is greater than 40mm, the power transfer efficiency significantly decreases with the increasing distance.

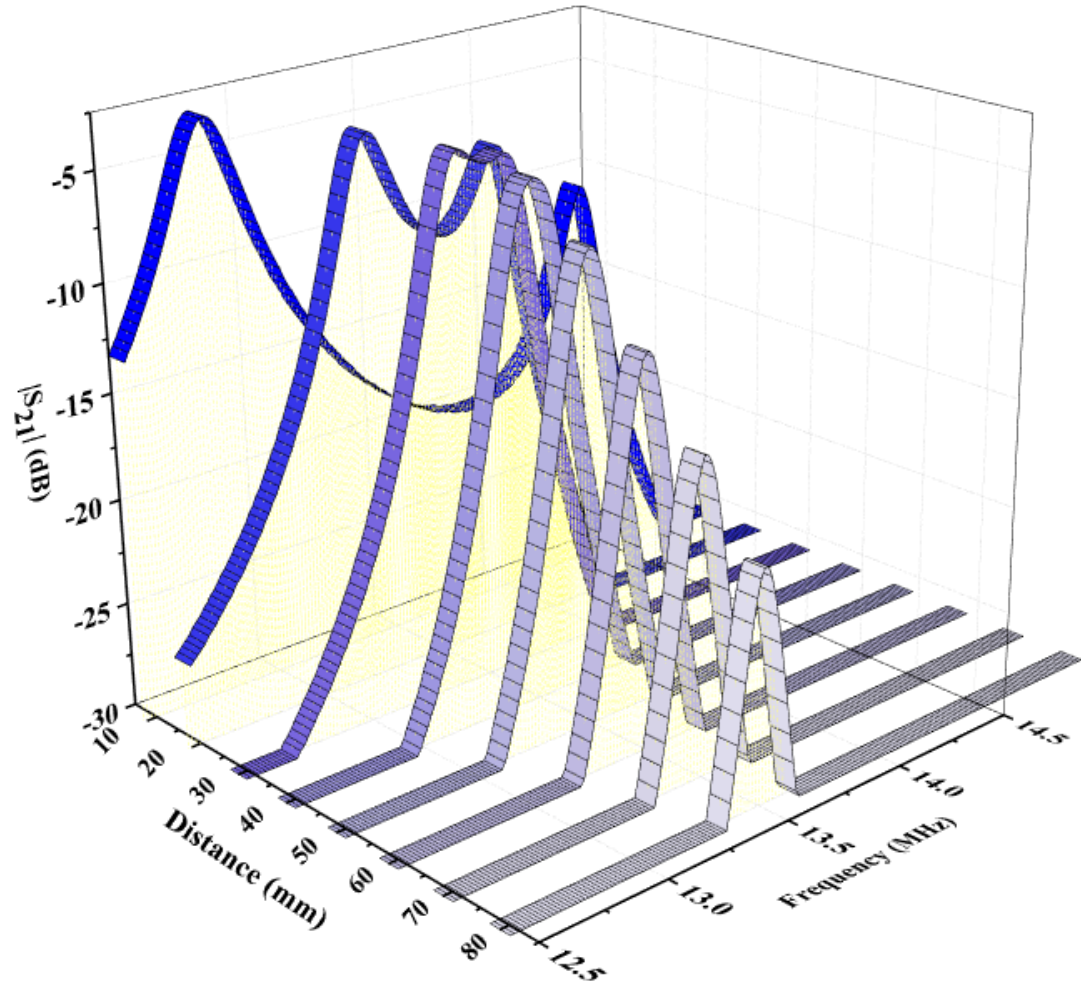


Figure 4-10: Measured power transfer efficiency of the proposed symmetric WPT system with ferrites when the distance between the transmitter and the receiver is changed from 10 mm to 80 mm.

4.3 Summary

In this chapter, a symmetric planar MCR-WPT system with size constraint of 32 mm^2 is proposed. The conventional planar MCR-WPT system is studied first and two ferrite structures (ferrite core and ferrite plates) are incorporated into the WPT system for performance improvement. Based on the measurement results, the power transfer

efficiency can be improved by 16.2%. The frequency splitting phenomenon is observed in the end to better understand the over coupled condition for a MCR-WPT system.

CHAPTER 5 THE PLANAR ASYMMETRIC MCR-WPT SYSTEM

The power transfer efficiency and transmission distance of the symmetric MCR-WPT system proposed in Chapter 4 was limited due to the small size of both transmitter and receiver coils. In this chapter, a large transmitter is presented to extend the power transfer range as well as the efficiency while the receiver size remains the same; they form the proposed asymmetric MCR-WPT system. Besides, an auxiliary copper strip is added to the receiver to increase self-inductance and mutual inductance. Moreover, influences of the nearby metallic objects for the WPT system will be investigated. By plotting the electromagnetic field distributions, ferrite materials can be shown capable of effectively reducing the impact of conductive objects. Finally, a planar asymmetric MCR-WPT system will be proposed in this chapter. The receiver size remains 32 mm^2 while transmitter size increases to 200 mm^2 . Different ferrite components are incorporated to improve system performances with respect to magnetic field leakages and EMI. The system is optimized using HFSS and fabricated as well with simulated and measured results show in section 5.2.

5.1 Design

5.1.1 Efficiency Improvement by Auxiliary Strips

An additional PSC printed on the back of the receiver substrate was proposed and

investigated in [13]; it improved the Q factor and power transfer efficiency. This technique is now applied to the asymmetric WPT system. By applying the auxiliary PSC or strip on the back of the receiver substrate proposed in Chapter 4, the same effect as adding a new turn can be achieved without increasing the size of the receiver. The simulated results show that the $|S_{21}|$ with or without the auxiliary strip are -2.86 dB and -3.75 dB, respectively, as shown in Figure 5-1, with other geometric parameters unchanged.

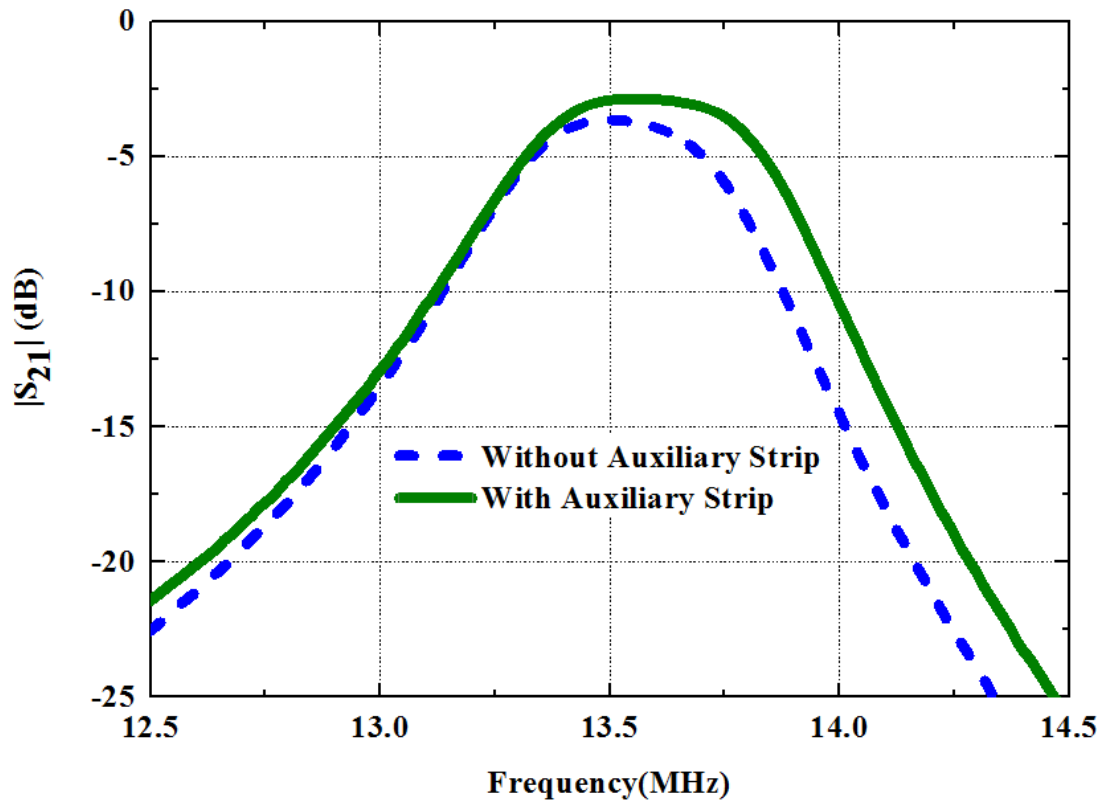


Figure 5-1: Measured $|S_{21}|$ of the proposed asymmetric WPT system receiver with and without auxiliary strip at the distance of 60 mm between the transmitter and receiver.

5.1.2 The Proposed System

As indicated before, a larger transmitter is employed in the proposed system as it will increase the magnetic flux intensity of the magnetic field being transmitted and improve the power transfer distance as well as transfer efficiency. The proposed transmitter is optimized using the same method as that described in Chapter 4. The final geometry is depicted in Figure 5-2. The geometric parameters and capacitor value are listed in Table 5-1.

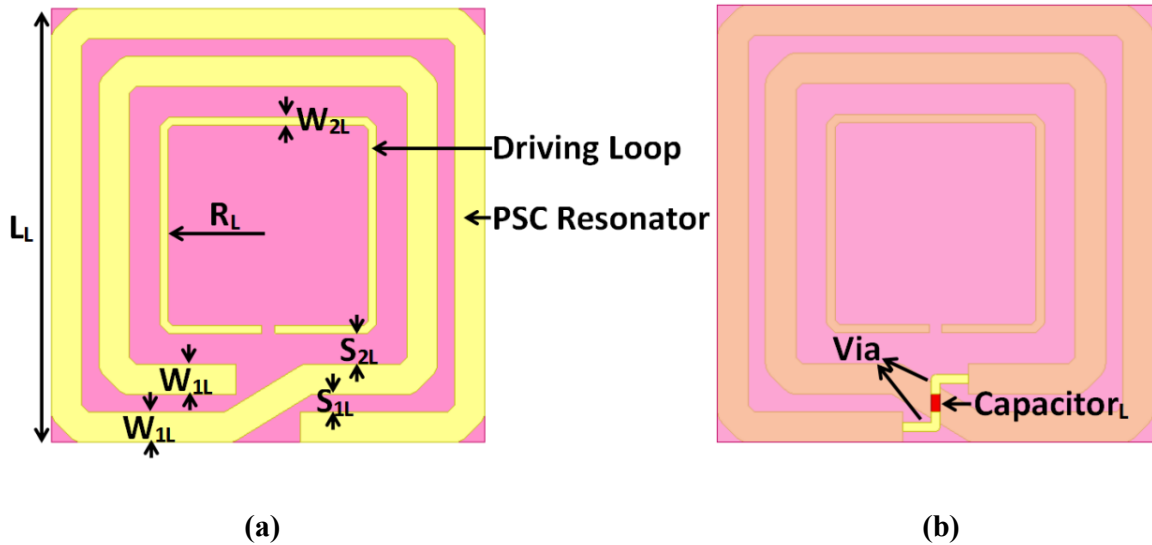
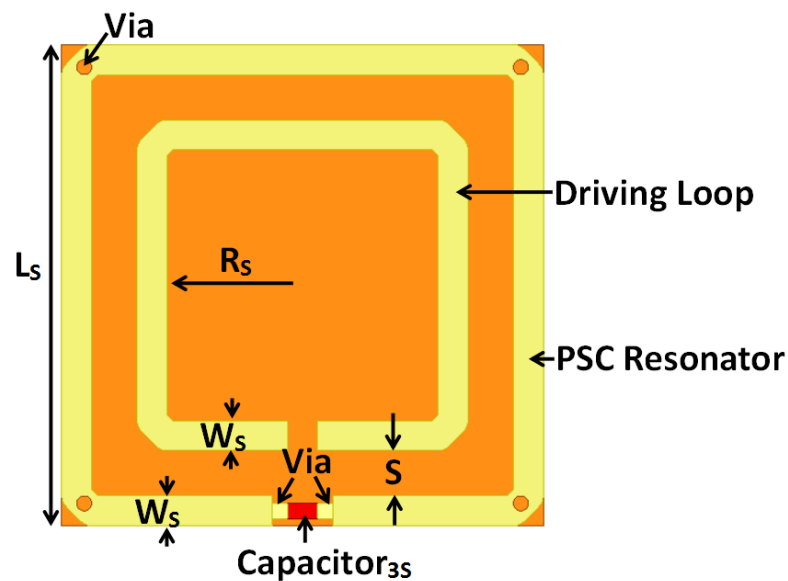


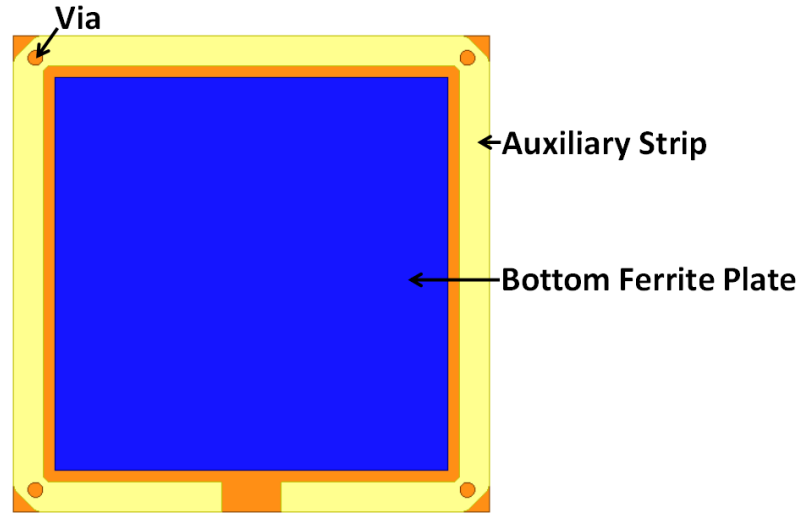
Figure 5-2: Geometry of the proposed asymmetric WPT system transmitter; (a) front view and (b) back view.

Due to a relatively large transmitter size, the small central ferrite core mounted on the receiver only shows an improvement of power transfer efficiency $|S_{21}|$ by about 0.1dB. Therefore, it is taken off as it increases the cost and complexity of the receiver. Only the ferrite plate is attached to the bottom of the receiver and the auxiliary strips are employed

to improve the performances.

The optimized asymmetric system geometry of the receiver with the auxiliary strip is depicted in Figure 5-3. The receiver dimension is $32 \times 32 \times 2.91$ mm. The PSC on the top of the receiver substrate is connected with the auxiliary strip on the back through four vias located in each corner of the resonator. The bottom ferrite plate is attached in the middle of the back of the receiver and has a dimension of $26.42 \times 26.42 \times 1.91$ mm. The capacitor is 2 nF at 13.56 MHz. The geometric parameters as well as capacitor values are listed in Table 5-1.





(b)

Figure 5-3: Structure of the proposed asymmetric WPT system receiver; (a) front view, (b) back view.

Table 5-1: Design parameters for asymmetric MCR-WPT system

| Receiver | | Transmitter | |
|------------------------------|------------------|-----------------------------|-----|
| $L_s(\text{mm})$ | 32 | $L_L(\text{mm})$ | 200 |
| $W_s(\text{mm})$ | 2 | $W_{1L}(\text{mm})$ | 14 |
| $S(\text{mm})$ | 3 | $W_{2L}(\text{mm})$ | 4 |
| $R_s(\text{mm})$ | 9 | $S_{1L}(\text{mm})$ | 8 |
| Capacitor _{3s} (nF) | 2 | $S_{2L}(\text{mm})$ | 14 |
| Bottom Ferrite Plate (mm) | 26.42×26.42×1.91 | $R_L(\text{mm})$ | 46 |
| | | Capacitor _L (pF) | 120 |

The overall asymmetric MCR-WPT system is shown in Figure 5-4, where d is the transfer distance. The center points of the transmitter and the receiver are aligned with each other.

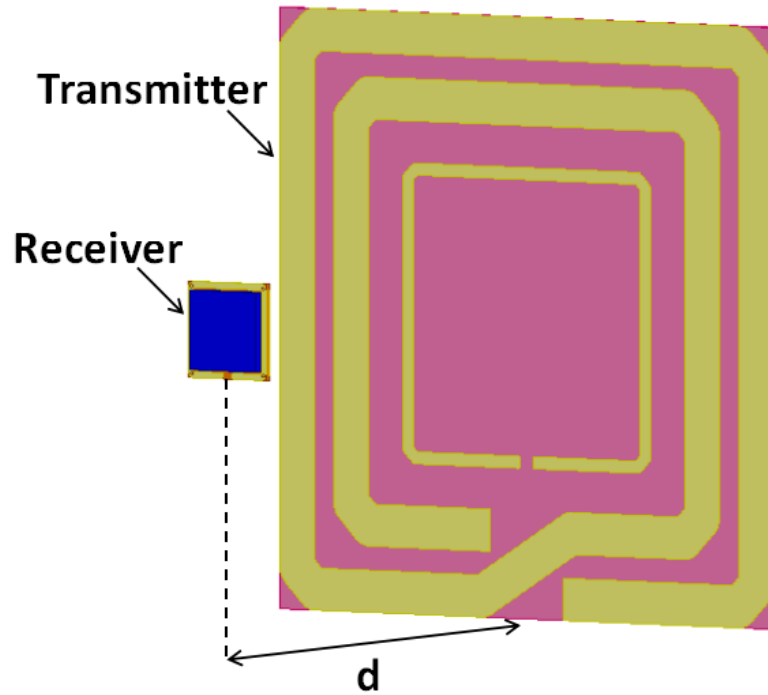


Figure 5-4: Overview of the proposed asymmetric WPT system

5.2 Results

The simulated results of the transfer efficiency under the optimal transmission condition with respect to four scenarios (one-turn PSC without auxiliary strip, one-turn PSC with auxiliary strip, two-turn PSCs without auxiliary strips and two-turn PSC with auxiliary strips) are listed in Table 5-2.

Table 5-2: Simulated power transfer efficiency with different turns of the receiver PSC and in the presence of auxiliary strip presented or not

| Transfer Efficiency (%) Number of Turns | With Auxiliary Strip | Yes | No |
|--|----------------------|------|------|
| | 1 | 52.0 | 44.5 |
| 2 | 45.9 | 36.7 | |

The auxiliary strip can improve the power transfer efficiency by 7.5 % based on the simulation results on one-turn PSC. The transfer efficiency of 52% is achieved by the receiver structure with one-turn PSC and auxiliary strip. The reason why the two-turn copper coil result in the lower efficiency is due to the increased parasitic capacitance.

The asymmetric system transmitter and receiver are optimized with HFSS and fabricated as shown in Figure 5-5. The supports are made by wood and foam, which will not electrically affect the power transfer over the distance since the transfer is carried out by magnetic fields. At the operational frequency of 13.56 MHz, the simulated and measured optimal distance is 60 mm, which is about twice of the receiver size.



Figure 5-5: The optimized asymmetric WPT system and the test setup.

The measured $|S_{11}|$ and $|S_{21}|$ of the optimized asymmetric MCR-WPT system is shown in Figure 5-6. The dip in the $|S_{11}|$ curve shows that the system resonates at 13.56 MHz. The $|S_{21}|$ can reach -2.86 dB, better than -4.8 dB of the symmetric system proposed in the previous chapter; a nearly 2 dB improvement is achieved with the asymmetric system. The corresponding measured maximum transfer efficiency is 51.8%, which is 18.7% improved

from that of the symmetric system.

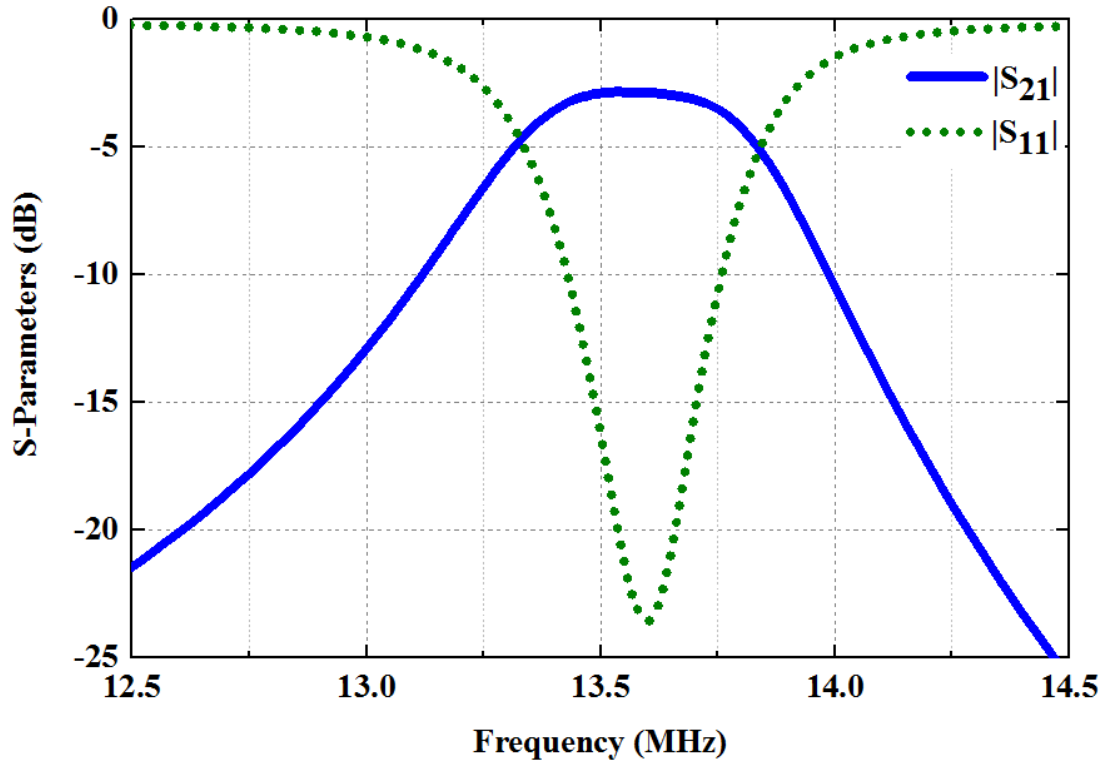


Figure 5-6: The measured $|S_{11}|$ and $|S_{21}|$ of the optimized asymmetric WPT system at 13.56 MHz with the distance of 60mm between the transmitter and receiver.

The measured and simulated power transfer efficiency of the proposed asymmetric WPT system are depicted and compared in Figure 5-7. The maximum transfer efficiency is 51.8% by measurement and 52% by simulation, respectively. The small differences are because of fabrication errors as well as non-ideal printed circuit boards and capacitors used.

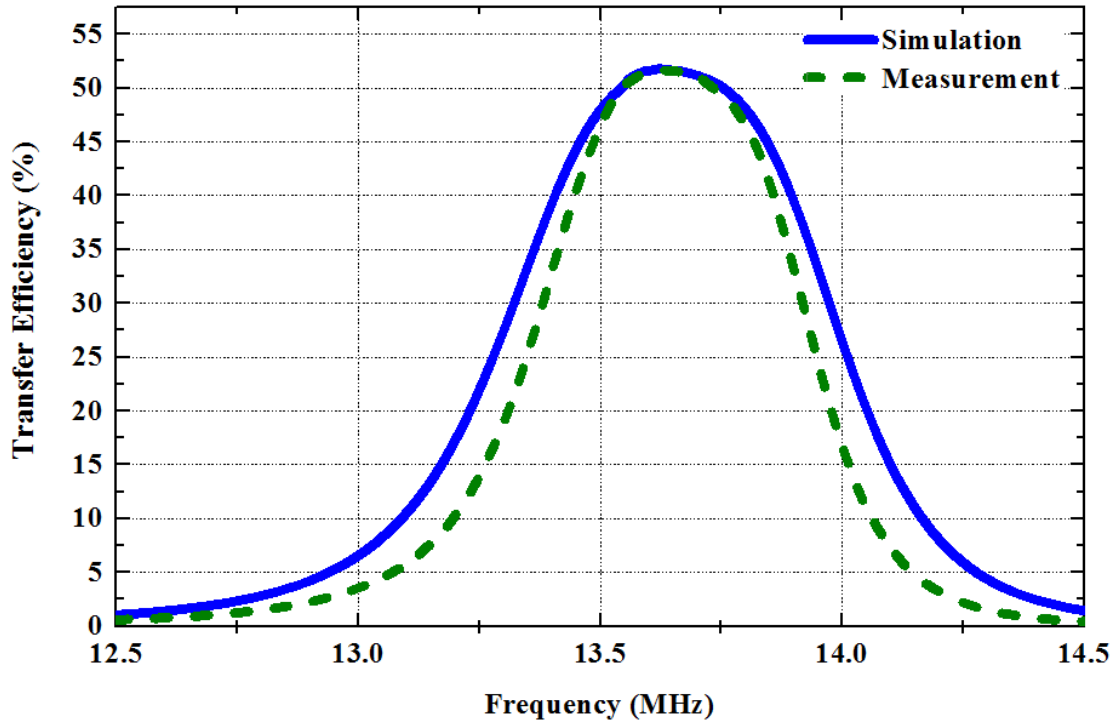


Figure 5-7: Measured and simulated power transfer efficiency of the proposed asymmetric WPT system at 13.56 MHz with 60 mm air gap.

Moreover, $|S_{21}|$ is shown at different positions of the receiver in the plane that is 60 mm away from the transmitter as shown in Figure 5-8. The result shows that $|S_{21}|$ is smoothly decreased from the central point (where the transmitter and the receiver is axially aligned) to the edges (where the transmitter and receiver is completely axially misaligned). The overall lateral misalignment performance shows that the proposed system can provide quite smooth power transfer within the cover area of the transmitter size.

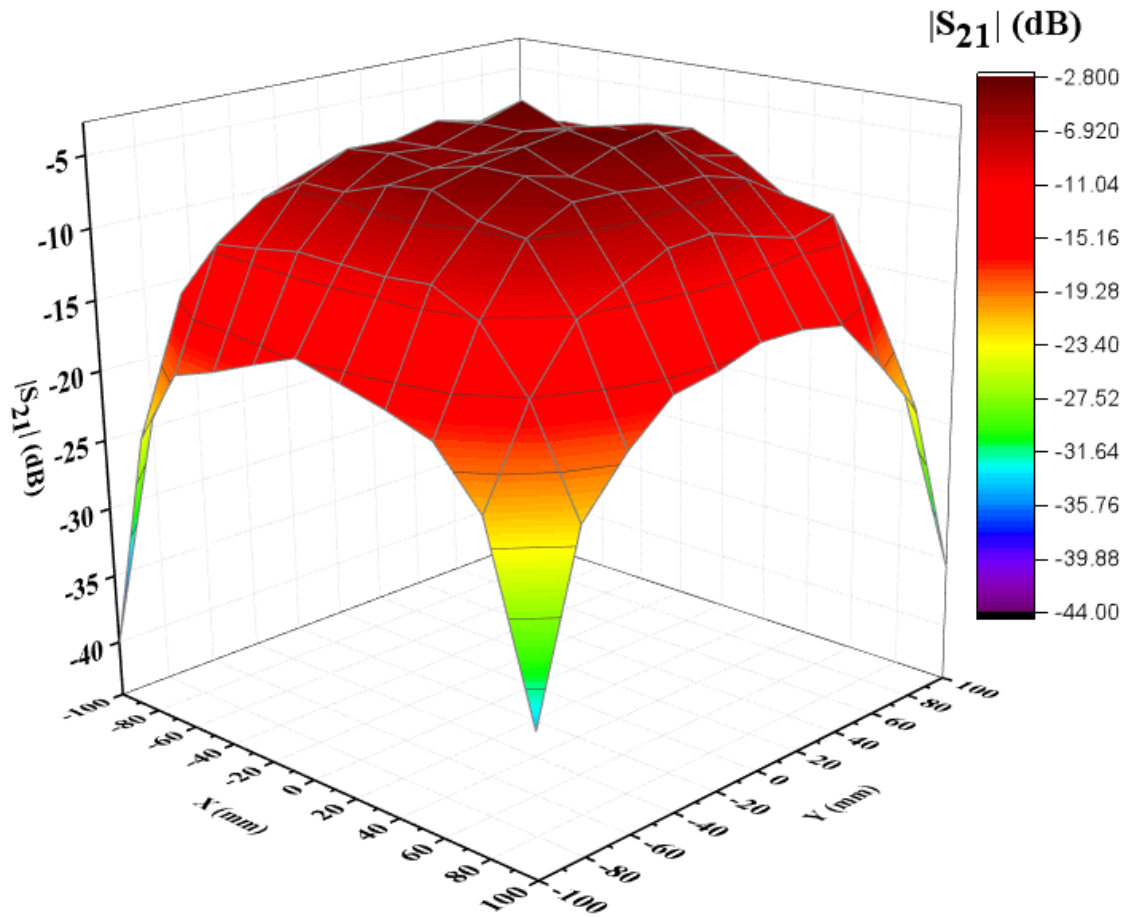


Figure 5-8: The S_{21} performance when directional misalignment of the optimized asymmetric WPT system.

The proposed asymmetric system is tested to power an LED bulb wirelessly. The experiment set up is shown in Figure 5-9. A power amplifier provides the power of 5 W to the transmitter.

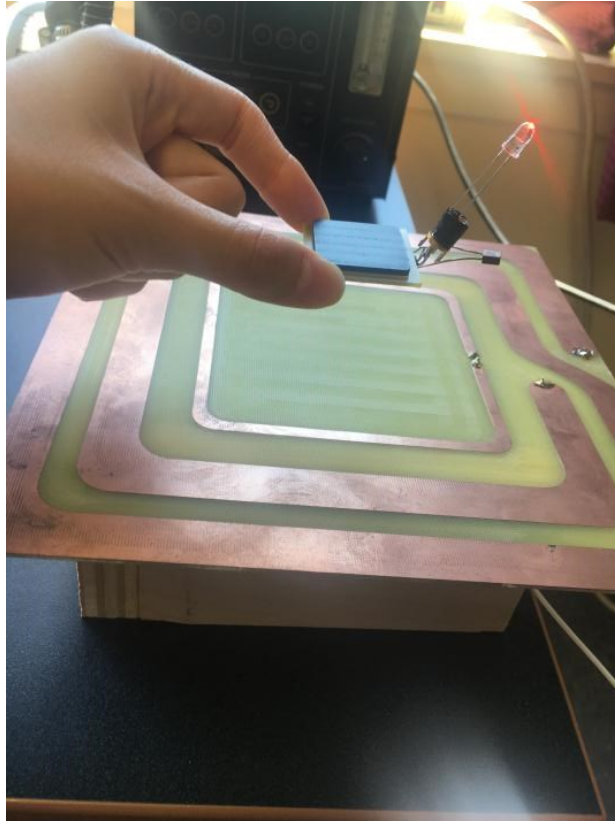


Figure 5-9: Experiment of lighting up an LED bulb wirelessly using the proposed asymmetric system

5.3 Effects of Conductive Object and Shielding Ferrite

5.3.1 Effects of Conductive Objects

A large amount of small electronic devices are encased by metals such as cell phones, tablets, and laptops. Since a WPT receiver needs to be embedded in the back of mobile devices or attached to the back [19], metals then act like shields that reduce magnetic fields at the receiver or even prevent the transmitted magnetic fields from reaching the receiver. This is because the skin depths of the metals are much smaller than the thickness of metals

at a high frequency.

To address this problem, camera lens on almost every cell phone were utilized in [10] to pass through magnetic fields and they are further studied here. The electromagnetic field distributions on a metal body with a camera hole is simulated with the metal dimensions of 142.5×69.5 mm (same as the Samsung Galaxy s7). The camera opening on the metal sheet can still block magnetic flux flowing into the receiver since the induced current around the camera hole can flow in a closed loop and produces counter magnetic fields [10]. Hence, a vertical slot is introduced from the camera hole to the edge of the metal cover to block the formation of the closed loop current. The geometry of the aluminum sheet with a camera opening and another aluminum sheet with the opening as well as the vertical slot are shown in Figure 5-10. The electromagnetic field distributions are presented in Figure 5-11. The results show that a substantially greater magnetic field on the metal sheet was created with the slot and the camera hole than that only with the camera hole.

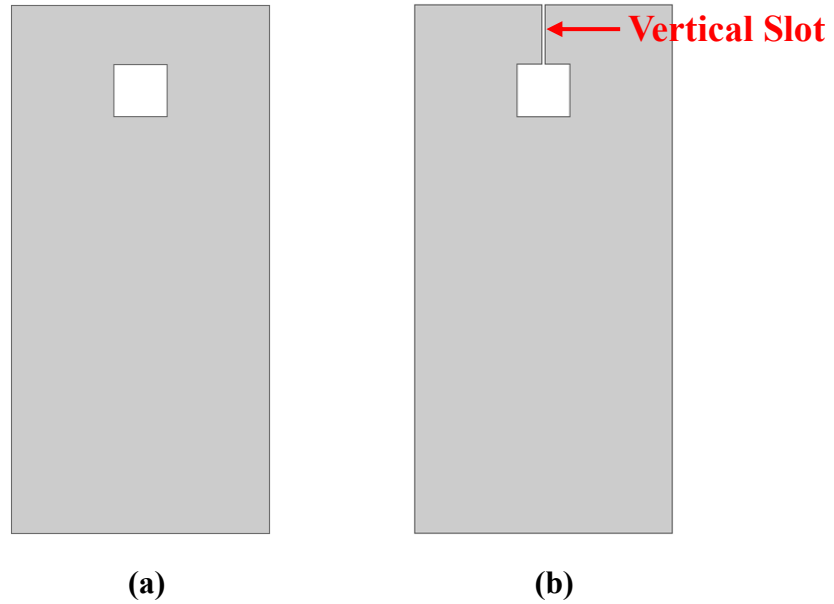


Figure 5-10: Headsets-sized medal sheet representing the back cover of a cell phone; (a) with the camera hole in the middle, (b) with the camera hole and the vertical slot.

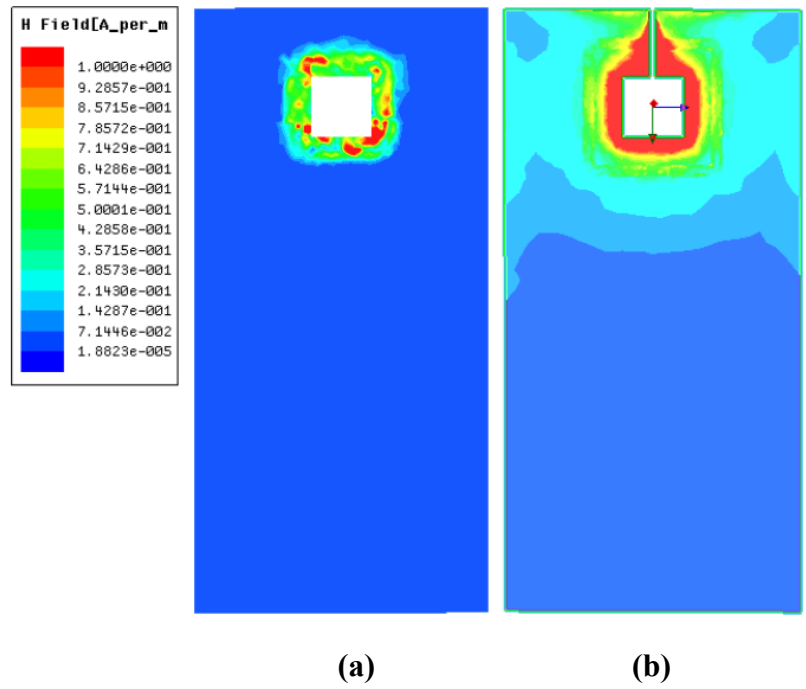
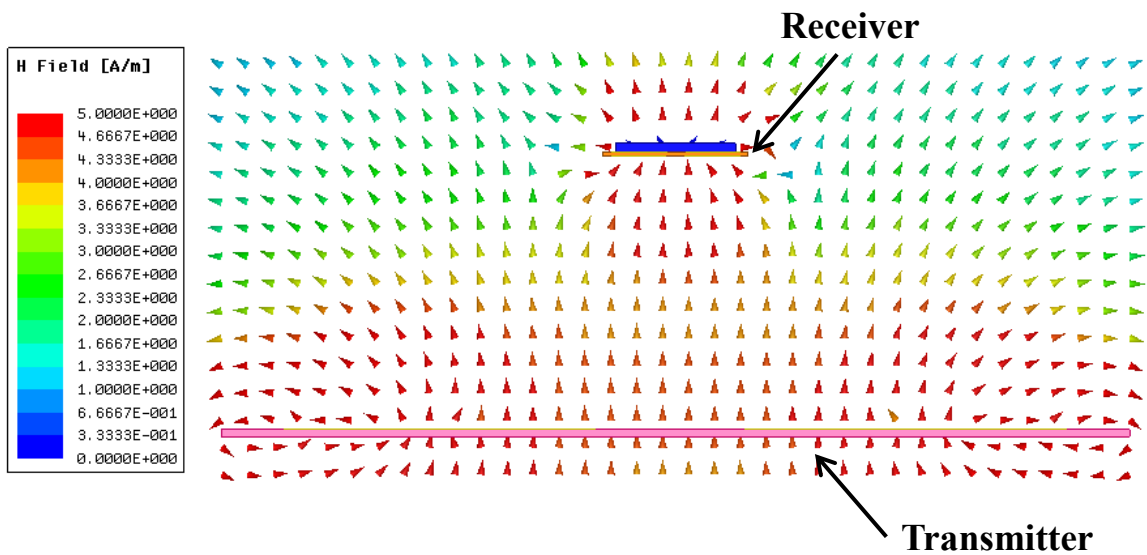


Figure 5-11: Induced eddy current on the medal sheet; (a) without vertical slot, (b) with vertical slot.

5.3.2 Effect of Shielding Ferrite Sheet

A ferrite sheet is applied further in the WPT system to mitigate the shielding problem at the receiver end. A ferrite sheet with size of $50 \times 40 \times 0.35$ mm is placed behind the receiver with distance of 5 mm to investigate its influence on the proposed system. The simulated electromagnetic field distributions with and without the ferrite sheet are shown Figure 5-12. A significantly reduced magnetic leakage and a more confine magnetic flux can be observed when the ferrite sheet is presented.



(a)

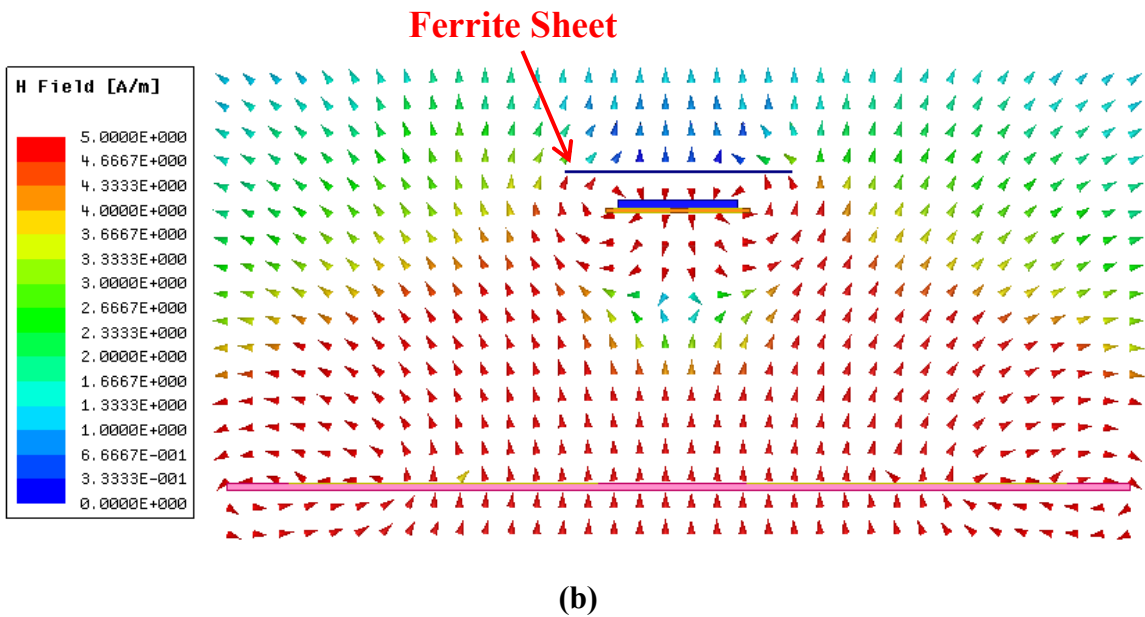
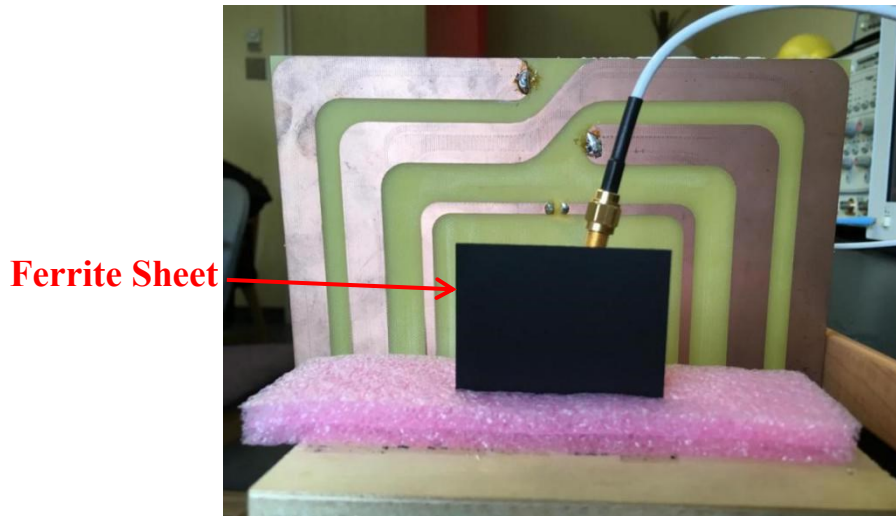


Figure 5-12: Electromagnetic field distribution when ferrite sheet placed near asymmetric WPT system or not; (a) without ferrite sheet, (b) with ferrite sheet.

The shielding ferrite plays another role to reduce impact of conductive objects like battery and metal cases. Figures 5-13 to 5-15 are the investigation set up of three scenarios: the asymmetric WPT system receiver and a ferrite sheet placed behind but at the distance of 5 mm (Figure 5-13), the receiver and an aluminum sheet placed behind but at the distance of 5 mm ((Figure 5-14), the receiver and both aluminum and ferrite sheet attached together placed behind the receiver but at the distance of 5 mm (Figure 5-15). The aluminum sheet has a size of 62×59 mm, larger than that of the ferrite; it is attached behind the ferrite sheet in the third scenario to simulate the situation in reality when the receiver is implanted into the metal phone case.

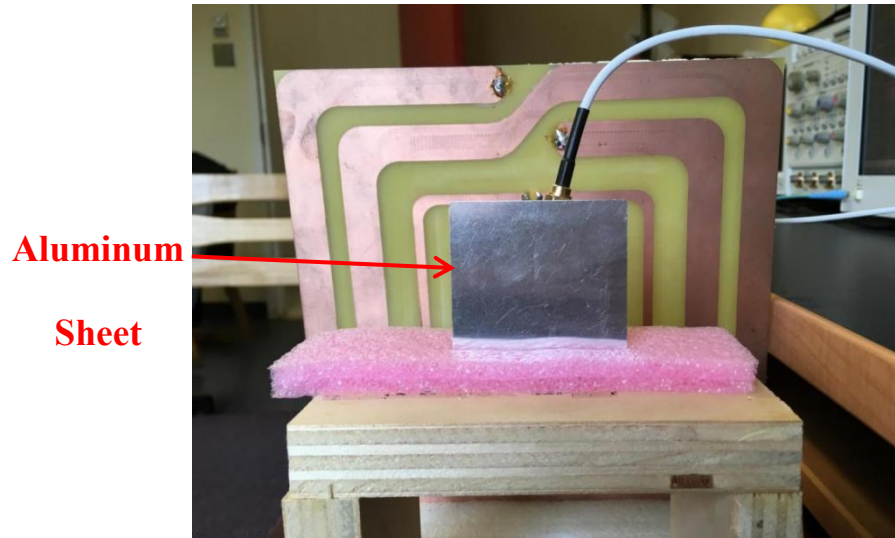


(a)



(b)

Figure 5-13: Measurement set up to test influences of the ferrite sheet on the asymmetric WPT system: (a) front view and (b) over view.



(a)



(b)

Figure 5-14: Measurement set up to test the influences of ferrite sheet on the asymmetric WPT system; (a) front view and (b) over view.

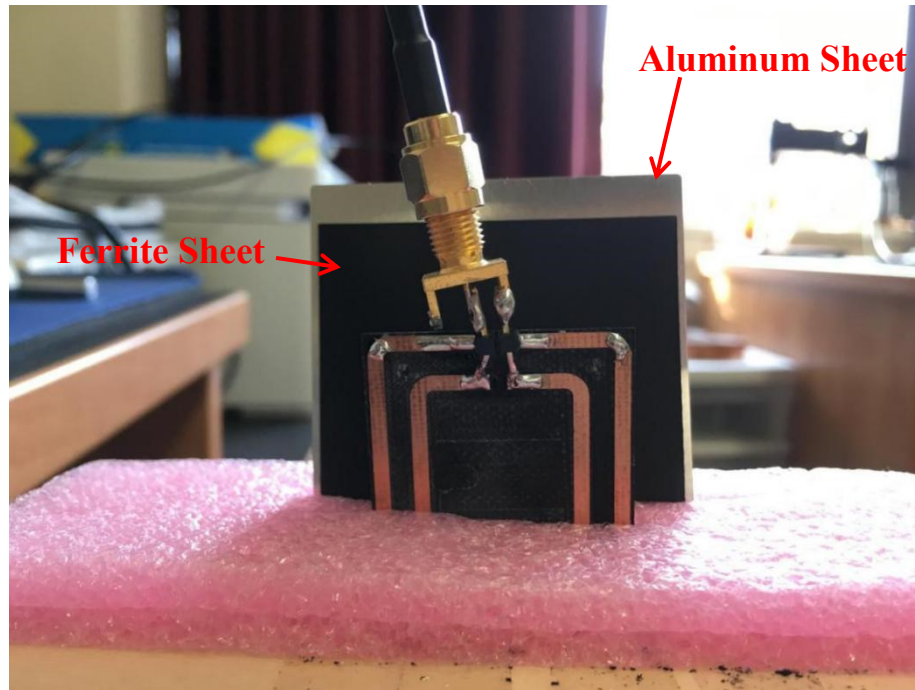


Figure 5-15: Measurement set up to test the effects of both metal (aluminum) and ferrite sheets placed behind the receiver.

The measurement results of $|S_{11}|$ and transfer efficiency are depicted in Figures 5-16 and 5-17. The frequency shifting phenomenon can be observed in $|S_{11}|$ and transfer efficiency when only the ferrite or aluminum sheet are present in the system. This is because the change of system configurations affects the system inductance. As can be seen from transfer efficiency curve, the power transfer efficiency drops by 10% when the aluminum sheet is present. However, when both ferrite and aluminum sheets are placed, transfer efficiency has almost the same results as those without the ferrite and aluminum sheet (with the peak values of 51.6% and 51.7% respectively). This means that the ferrite sheet can effectively mitigate the impacts of nearby mantellic objects.

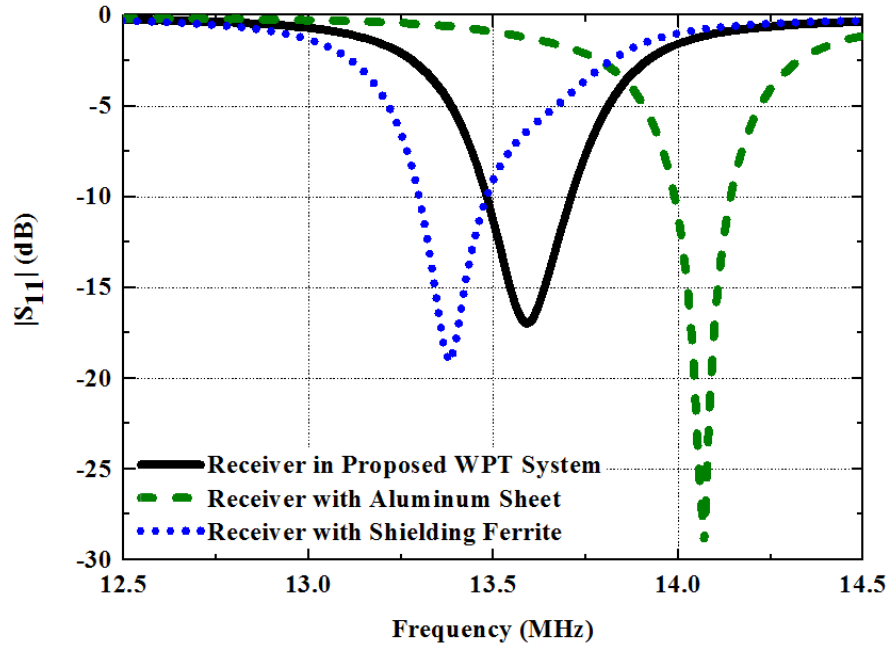


Figure 5-16: The measured $|S_{11}|$ of the proposed asymmetric WPT system with ferrite or aluminum sheet near the receiver.

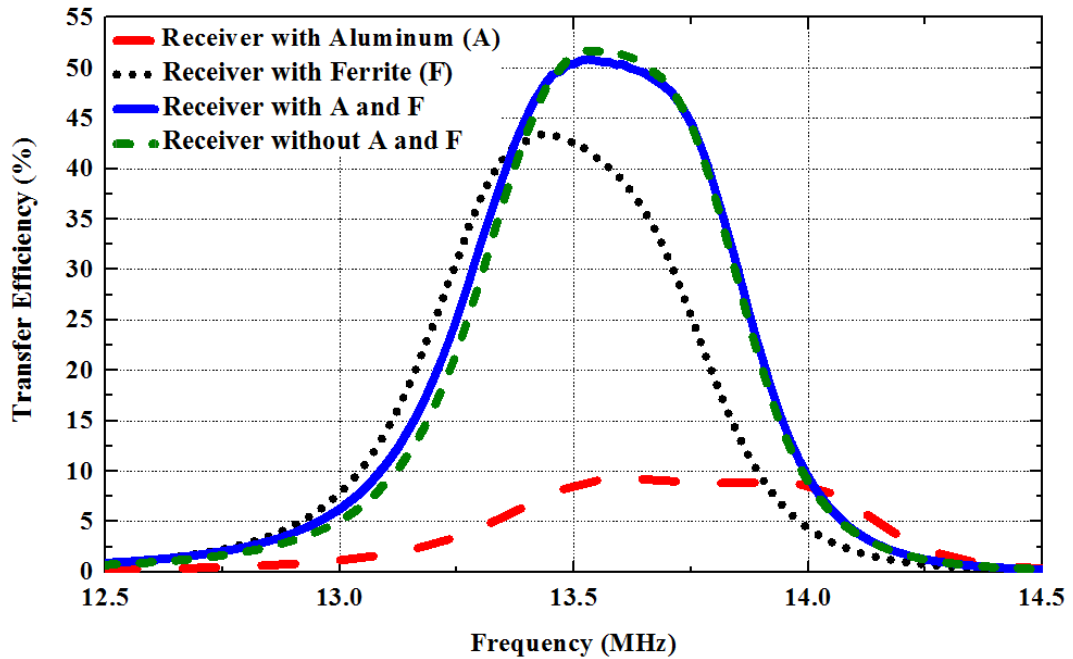


Figure 5-17: The measured transfer efficiency of the proposed asymmetric WPT system with ferrite or aluminum sheet or both nearby the receiver in comparison with the receiver only.

The three ferrite components being used in the thesis with their names and functions are summarized in Table 5-3.

Table 5-3: Summing up different ferrite sizes and functions

| Name | Volume (mm³) | Photograph | Function |
|------------------------------------|--------------------------------|--|--|
| Central Ferrite Core | 8×8×2 |  | Confine magnetic field |
| Bottom Ferrite Plate | 26.42×26.42×1.91 |  | Confine magnetic field, mitigate magnetic leakage |
| Shielding Ferrite Sheet | 50×40×0.35 |  | Mitigate magnetic leakage, shield magnetic interference |

5.4 Summary

A planar asymmetric MCR-WPT system was proposed in this chapter with both simulation and measurement results. The effects of ferrites and metal sheets on system performances are studied and investigated. The results show that different from the ferrite core and ferrite plate, the ferrite sheet can dramatically mitigate magnetic field leakages and shield electromagnetic interferences and other effects by nearby metallic objects. Since

existence of conductive materials is inevitable in cell phones and other electronic devices, shielding ferrite sheets can be applied to the WPT system to improve the system performance. Properties of the three ferrite structures incorporated into the symmetric and asymmetric MCR-WPT systems are summarized and shown in this chapter.

CHAPTER 6 CONCLUSION AND FUTURE WORK

6.1 Conclusion

The objective of this thesis is to develop WPT systems for small electronic devices. The magnetically coupled resonance method is chosen to achieve the goal because of its suitability for low-power and small-size applications with space freedom. The existing WPT systems for consumer electronic devices are discussed with their advantages and disadvantages described. There is a need for practical WPT systems that can provide a good power transfer efficiency over the specific area and that is of smaller sizes for consumer electronic devices. Two MCR-WPT systems are proposed in this thesis. They are designed to take advantages of the previously proposed systems and avoid their disadvantages. They can achieve the high power transfer efficiency within the size constraint of $32 \times 32 \times 3.91$ mm (L×W×H).

The design methods are discussed in chapter 3, with the equivalent circuit models for the structures without ferrite materials first to better understand how the design parameters affect the system performances. Because of the non-linear and complex properties of ferrite materials, numerical method is then used to simulate the structures. The effects of ferrite materials in improving WPT system performances are studied and presented.

The symmetric MCR-WPT system is proposed and it has small transmitter and receiver size of $32 \times 32 \times 3.91$ mm. Because of the low power transfer efficiency with small WPT transmitters and receivers, central ferrite core and bottom ferrite plate are applied and they

result in a 32.8 % power transfer efficiency at a transmission distance of 35 mm. The system can be used in charging cell phones with portable power supply.

To further improve the power transfer efficiency, the asymmetric MCR-WPT system is proposed. A relatively large transmitter with size of $200 \times 200 \times 1.6$ mm is first developed without ferrite materials. The receiver size remains small which is $32 \times 32 \times 2.91$ mm, so it can be built into consumer electronics such as cell phones. The auxiliary strip is added to the receiver to increase the Q factor of the receiving coil resonator and thus improve the transfer efficiency as well as the charging distance to 51.8 % and 60 mm respectively. The proposed system is suitable for mobile phone recharging. Finally, the effects of ferrite and aluminum sheets on the proposed systems are measured and analyzed.

In summary, the work done in this thesis is (1) innovative in the transmitter and receiver structures design, (2) rigorous in validation and comparison between simulation and measurement results, and novel in incorporating ferrites into the WPT systems. Overall, the proposed systems are good candidates for wirelessly charging small electronic devices.

6.2 Future Work

In consideration of the general challenges of the WPT techniques for small electronic devices, much future works can still be done based on the work presented in this thesis.

They are as follows:

- Matching design: inductance values of the proposed transmitter and receiver coils are sensitive to charging distance, alignment angles and presence of foreign objects.

They lead to the difficulty of tuning the resonant frequency. A particular matching design could be considered in the future to make the tuning adaptive.

- **Coil topologies:** the focus of this work is on the transmitter and receiver design. Further research can be on other coil structures. For instance, serially connected auxiliary coils may improve system performances and multi-loop feed concept may be further explored.
- **Materials:** ferrite materials are studied and found beneficial for WPT in this thesis. Other materials, such as metamaterials, can be explored further. Not only the structure configurations of new materials but also the ways they are incorporated into the WPT systems as well as theoretical analyses can be investigated further.
- **Multi-receiver charging:** since one person can have many small electronics, such as mobile phones, wireless speakers, laptops and iPads, they may need to be charged at the same time. Therefore, it will be good to develop a WPT system that can carry out charging of multiple receivers at the same time. Although a couple of multi-receiver systems have been proposed [15] using transmitting coil array, further work is still needed to improve the efficiency.
- **Multi-functions integration:** many useful functions may be combined and integrated into the WPT systems. For instance, data communication may be integrated into a WPT system so that a WPT system can achieve both data and power transfer at the same time.

REFERENCES

- [1] A. Kursl, A. Karalis, R. Moffattl, J. D. Joannopoulos, P. Fisher and M. Soljačić, “Wireless power transfer via strongly coupled magnetic resonances,” *Science Magazine*, vol.317, no. 5834, pp. 83-86, 2007.
- [2] P. Zuo, X. Wu, W. Li, W. Liu, “Design of Wireless Energy Transfer System Based on Coupled Magnetic Resonances”, *IEEE International Conference on Aircraft Utility Systems (AUS)*, pp. 527 – 532, 2016.
- [3] A. P. Sample, D. T. Meyer and J. R. Smith, “Analysis, Experimental Results, and Range Adaption of Magnetically Coupled Resonators for Wireless Power Transfer”, *IEEE Transactions on Industrial Electronics*, vol. 52, pp. 544-554, 2011.
- [4] Z. Luo, X. Wei, “Analysis of Square and Circular Planar Spiral Coils in Wireless Power Transfer Systems for Electric Vehicles”, *IEEE Transactions on Industrial Electronics*, vol. 65, pp. 331 - 341, 2018.
- [5] S. Li, C. C. Mi, “Wireless Power Transfer for Electric Vehicle Applications”, *IEEE Journal of Emerging and Selected Topics in Power Electronics*, vol. 3, pp. 4 - 17, 2015.
- [6] H. Kim, C. Song, J. Kim, D. H. Jung, E. Song, S. Kim, J. Kim, “Design of magnetic shielding for reduction of magnetic near field from wireless power transfer system for electric vehicle”, *International Symposium on Electromagnetic Compatibility*, pp. 53 - 58, 2014.

- [7] H. Hee Lee, S. H. Kang, C. W. Jung, “3D-spatial efficiency optimisation of MR-WPT using a reconfigurable resonator-array for laptop applications”, *IET Microwaves, Antennas & Propagation*, vol. 11, pp. 1594 - 1602, 2017.
- [8] F. Jolani, J. Mehta, Y. Yu, Z. Chen, “Design of Wireless Power Transfer Systems Using Magnetic Resonance Coupling for Implantable Medical Devices”, *Progress In Electromagnetics Research Letters*, vol. 40, pp. 141 - 151, 2013.
- [9] S. Hached, A. Trigui, I. E. Khalloufi, M. Sawan, O. Loutochin, J. Corcos, “A Bluetooth-based Low-Energy Qi-compliant battery charger for implantable medical devices”, *IEEE International Symposium on Bioelectronics and Bioinformatics (IEEE ISBB)*, pp. 1 - 4, 2014.
- [10] N. S. Jeong and F. Carobolante, “Wireless charging of a metal-body device,” *IEEE Journals and magazines*, vol. 65, pp. 1077 - 1086, 2017.
- [11] F. Jolani, Y. Yu and Z. Chen, “A Planar Magnetically Coupled Resonant Wireless Power Transfer System Using Printed Spiral Coils,” *IEEE Antennas and Wireless Propagation Letters*, vol. 13, pp. 1648–1651, 2014.
- [12] F. Jolani, Y. Yu and Z. Chen, “A novel planar wireless power transfer system with strong coupled magnetic resonances,” *IEEE International Wireless Symposium*, pp. 1-4, 2014.
- [13] F. Jolani, Y. Yu and Z. Chen, “Enhanced Planar Wireless Power Transfer Using Strongly Coupled Magnetic Resonance,” *Electronics Letters*, vol. 51, pp. 173-175, 2015.

- [14] Z. Liu, Z. Chen, J. Li and Y. Guo, "A planner L-shape transmitter for wireless power transfer system," *IEEE Journals & Magazines*, vol. 16, pp. 960 - 96, 2016.
- [15] Z. Liu, Y. Guo, F. Jolani, Y. Yu and Z. Chen, "Planar magnetically-coupled resonance wireless power transfer system using array of coil resonators," *IEEE conference publications*, 2016.
- [16] O. Jonah and S. V. Georgakopoulos, "Optimized Helix with Ferrite Core for Wireless Power Transfer via Resonance Magnetic," *IEEE Antennas and Propagation Society International Symposium*, pp. 1040-1041, 2013.
- [17] T. Batra, E. Schaltz and S. Ahn, "Reduction of Magnetic Emission by Increasing Secondary Side Capacitor for Ferrite Geometry based Series-Series Topology for Wireless Power Transfer to Vehicles," *16th European Conference on Power Electronics and Applications*, pp. 1-11, 2014.
- [18] H. Kim, C. Song, J. Kim, J. Kim and J. Kim, "Shielded Coil Structure Suppressing Leakage Magnetic Field from 100W-Class Wireless Power Transfer System with Higher Efficiency," *IEEE MTT-S International Microwave Workshop Series on Innovative Wireless Power Transmission*, pp. 83-86, 2012.
- [19] T. Kim, S. Yoon, J. Yook, G. Yun and W. Lee, "Evaluation of Power Transfer Efficiency With Ferrite Sheets in WPT System," *IEEE Wireless Power Transfer Conference (WPTC)*, pp. 1-4, 2017.
- [20] H. Park, J. Kwon, S. Kwak and S. Ahn, "Effect of Air-Gap Between a Ferrite Plate and Metal Strips on Magnetic Shielding," *IEEE Transactions on Magnetics*, vol. 51,

2015.

- [21] Y. Park, J. Kim, K. Kim, “Magnetically Coupled Resonance Wireless Power Transfer (MR-WPT) with Multiple Self-Resonators”, *Wireless Power Transfer - Principles and Engineering Explorations*, Dr. Ki Young Kim (Ed.), ISBN: 978-953-307-874-8, InTech, pp. 51-65, 2012.
- [22] IDT Global Trends, “Wireless power transfer system inventory – Did you get these points?”, 06/30 2016. https://mp.weixin.qq.com/s/_UMNc-TLsWLY6DJC54yt9A.
- [23] 23 K. Knaisch, M. Springmann, P. Gratzfeld, “Comparison of coil topologies for inductive power transfer under the influence of ferrite and aluminum”, *Eleventh International Conference on Ecological Vehicles and Renewable Energies (EVER)*, pp. 1 - 9, 2016.
- [24] M. Kim, J. Byeon, B. K. Lee, J. Lee, “Performance analysis of magnetic power pads for inductive power transfer systems with ferrite structure variation”, *IEEE Energy Conversion Congress and Exposition (ECCE)*, pp. 1 - 6, 2016.
- [25] N. Liu, B. Wang, “An LLC-based planar wireless power transfer system for multiple devices”, *IEEE Applied Power Electronics Conference and Exposition (APEC)*, pp. 3411 - 3417, 2014.
- [26] B. L. Cannon, J. F. Hoburg, D. D. Stancil, S. C. Goldstein, “Magnetically coupled resonance As a Potential Means for Wireless Power Transfer to Multiple Small Receivers”, *IEEE Transactions on Power Electronics*, vol. 24, pp. 1819 - 1825, 2009.
- [27] C. Song, H. Kim, D. H. Jung, J. J. Kim, S. Kong, J. Kim, S. Ahn, J. Kim, J. Kim,

- “Low EMF and EMI Design of a Tightly Coupled Handheld Resonant Magnetic Field (HH-RMF) Charger for Automotive Battery Charging”, *IEEE Transactions on Electromagnetic Compatibility*, vol. 58, pp. 1194 - 1206, 2016.
- [28] H. Mao, B. Yang, Z. Li, S. Song, X. Zhao, “Flexible and efficient 6.78MHz wireless charging for metal-cased mobile devices using controlled resonance power architecture”, *IEEE Wireless Power Transfer Conference (WPTC)*, pp. 1 - 4, 2017.
- [29] Q. Liu, J. Wu, P. Xia, S. Zhao, W. Chen, Y. Yang, L. Hanzo, “Charging Unplugged: Will Distributed Laser Charging for Mobile Wireless Power Transfer Work?”, *IEEE Vehicular Technology Magazine*, vol. 11, pp. 36 - 45, 2016.
- [30] X. Lu, D. Niyato, P. Wang, D. I. Kim, Z. Han, “Wireless charger networking for mobile devices: fundamentals, standards, and applications”, *IEEE Wireless Communications*, vol. 22, pp. 126 - 135, 2015.
- [31] X. Mou, H. Sun, “Wireless Power Transfer: Survey and Roadmap”, *IEEE 81st Vehicular Technology Conference (VTC Spring)*, pp. 1 - 5, 2015.
- [32] A. Steven. “Wireless recharging: Pulling the plug on electric cars”, 20/11 2012.
<http://www.bbc.com/future/story/20121120-pulling-the-plug-on-electric-cars>.
- [33] S. Beak, S. Choi, S. Rhee, S. Han, T. Jeong, “Energy charging circuits in Bluetooth environment for smart phone”, *IEEE International Conference on Consumer Electronics (ICCE)*, pp. 109 - 110, 2011.
- [34] N. Desai, A. P. Chandrakasan, “A ZVS resonant receiver with maximum efficiency tracking for device-to-device wireless charging”, *42nd European Solid-State Circuits*

- Conference*, pp. 313 - 316, 2016.
- [35] R. Kuo, P. Riehl, J. Lin, “3-D wireless charging system with flexible receiver coil alignment”, *IEEE Wireless Power Transfer Conference (WPTC)*, pp. 1 - 4, 2016.
- [36] H. Kim, C. Song, J. Kim, H. B. Park, H. H. Park, E. Song, J. Kim, “Optimization procedure of complex permeability for a wireless power transfer system”, *Asia-Pacific Symposium on Electromagnetic Compatibility (APEMC)*, pp. 1 - 4, 2013.
- [37] M. Treffers, “History, Current Status and Future of the Wireless Power Consortium and the Qi Interface Specification”, *IEEE Circuits and Systems Magazine*, vol. 15, pp. 28 - 31, 2015.
- [38] W. Li, P. Wang, C. Yao, Y. Zhang, H. Tang, “Experimental investigation of 1D, 2D, and 3D metamaterials for efficiency enhancement in a 6.78MHz wireless power transfer system”, *IEEE Wireless Power Transfer Conference (WPTC)*, pp. 1 - 4, 2016.
- [39] H. Kim, C. Song, J. Kim, J. Kim, J. Kim, “Shielded coil structure suppressing leakage magnetic field from 100W-class wireless power transfer system with higher efficiency”, *IEEE MTT-S International Microwave Workshop Series on Innovative Wireless Power Transmission: Technologies, Systems, and Applications*, pp. 83 – 86, 2012.
- [40] Z. N. Low, R. A. Chinga, R. Tseng, J. Lin, “Design and Test of a High-Power High-Efficiency Loosely Coupled Planar Wireless Power Transfer System”, *IEEE Transactions on Industrial Electronics*, vol. 56, pp. 1801 - 1812, 2009.
- [41] J. Farid, *Wireless Power Transfer Via Magnetically coupled resonance*, Halifax: 2015.

- [42] H. Son, J. Kim, D. Kim, K. Kim, Y. Park, “Self-resonant coil with coaxial-like capacitor for wireless power transfer”, *Asia-Pacific Microwave Conference*, pp. 90 - 93, 2011.
- [43] J. W. Nilsson, S. Riedel. *Electric Circuits* (9th Edition). New Jersey: Prentice Hall, 2011. Print.
- [44] K. J. Duncan, “Laser based power transmission: Component selection and laser hazard analysis”, *IEEE PELS Workshop on Emerging Technologies: Wireless Power Transfer (WoW)*, pp. 100 - 103, 2016.
- [45] R. Mehrotra, “Cut the Cord: Wireless Power Transfer, its Applications, and its limits”, 05/05 2014. <https://www.cse.wustl.edu/~jain/cse574-14/ftp/power.pdf>.
- [46] 46 W. C. Brown, “The History of Power Transmission by Radio Waves”, *IEEE Transactions on Microwave Theory and Techniques*, vol. 32, pp. 1230 - 1242, 1984.
- [47] J. Kim, H. Kim, C. Song, I. Kim, Y. Kim, J. Kim, “Electromagnetic interference and radiation from wireless power transfer systems”, *IEEE International Symposium on Electromagnetic Compatibility (EMC)*, pp. 171 - 176, 2014.
- [48] P. Kukreja, C. Berly, U. Kiran, “Wireless power transfer system using loop antenna and its gain enhancement using SRR metamaterial”, *Third International Conference on Advances in Electrical, Electronics, Information, Communication and Bio-Informatics (AEEICB)*, pp. 264 - 267, 2017.
- [49] A. Alphones, J. P. K. Sampath, “Metamaterial assisted wireless power transfer system”, *Asia-Pacific Microwave Conference (APMC)*, vol. 2, pp. 1 - 3, 2015.

- [50] Y. Cho, S. Lee, S. Jeong, H. Kim, C. Song, K. Yoon, J. Song, S. Kong, Y. Yun, J. Kim, “Hybrid metamaterial with zero and negative permeability to enhance efficiency in wireless power transfer system”, *IEEE Wireless Power Transfer Conference (WPTC)*, pp. 1 - 3, 2016.
- [51] A. G. Pelekanidis, A. X. Lalas, N. V. Kantartzis, T. D. Tsiboukis, “Optimized wireless power transfer schemes with metamaterial-based resonators”, *International Workshop on Antenna Technology: Small Antennas, Innovative Structures, and Applications (iWAT)*, pp. 289 - 292, 2017.
- [52] B. Park and J. Lee, “Enhanced Efficiency for Wireless Power Transmission Using An Auxiliary Loop on Ferrite in Metallic Environment,” *Electronics Letters*, vol. 51, pp. 2039-2041, 2015.
- [53] A. Robichaud, M. Boudreault, D. Deslandes, “Comparison between inductance topologies for resonant wireless power transmission applications”, *Asia Pacific Microwave Conference Proceedings*, pp. 397 - 399, 2012.
- [54] User’s guide - High Frequency Structure Simulator. Pittsburgh: Ansoft Corporation, 2005.
- [55] J. Park, D. Kim, K. Hwang, H. Park, S. Kwak, J. Kwon, S. Ahn, “A Resonant Reactive Shielding for Planar Wireless Power Transfer System in Smartphone Application”, *IEEE Transactions on Electromagnetic Compatibility*, vol. 59, pp. 695 - 703, 2017.
- [56] M. A. Javaid, K. L. Bhatti, Z. Raza, U. Ilyas and S. U. Haq, “Wireless power

- transmission ‘A potential idea for future’”, *International Journal of Scientific and Engineering Research*, vol. 6, 2015.
- [57] S. Assawaworrarit, X. Yu, S. Fan, “Robust wireless power transfer using a nonlinear parity-time-symmetric circuit”, *Nature Letters*, vol. 546, pp. 387-390, 2017.
- [58] S. Pu, H. T. Hui, “An efficient wireless power transmission system by employing 3×3 stacked coil antenna arrays”, *IEEE International Conference on RFID Technology and Applications (RFID-TA)*, pp. 171 - 175, 2015.
- [59] B. M. Badr, R. S. Gsizmazia, K.R. Delaney, N. Dechev, “Wireless Power Transfer for Telemetric Devices With Variable Orientation, for Small Rodent Behavior Monitoring”, *IEEE Sensors Journal*, vol. 15, pp. 2144 - 2156, 2015.
- [60] A. Tejada, C. Carretero, J. T. Boys, G. A. Covic, “Ferrite-Less Circular Pad With Controlled Flux Cancellation for EV Wireless Charging”, *IEEE Transactions on Power Electronics*, vol. 32, pp. 8349 - 8359, 2017.
- [61] S. Mukherjee, “Mitigation of proximity to metal for magnetically coupled transponders by use of resonant loops”, *IEEE International Conference on RFID (IEEE RFID)*, pp. 8 - 14, 2014.
- [62] J. Park, K. Hwang, D. Kim, S. Ahn, “Lateral misalignment tolerance enhancement by using electromagnet based flux gate in wireless power transfer systems”, *IEEE Wireless Power Transfer Conference (WPTC)*, pp. 1 - 4, 2016.
- [63] S. M. Khan, “Analysis of wireless power transfer (WPT) scheme with connected ground planes”, *USNC-URSI Radio Science Meeting (Joint with AP-S Symposium)*,

pp. 21 - 22, 2017.

- [64] R. Feng, D Czarkowski, F. Leon, K. Mude, “Optimal design of resonant coupled multi-receiver wireless power transfer systems”, *IEEE International Conference on Industrial Technology (ICIT)*, 1561 - 1566, 2017.
- [65] Z. Lu, W. W. Li, Y. Pang, M. Pan, W. Wu, Z. Han, “Collaborative Data and Energy Transmission for Energy-Rechargeable Mobile Devices”, *IEEE Transactions on Wireless Communications*, vol 15, pp. 8525 - 8536, 2016.
- [66] A. Satyamoorthy, P. Riehl, H. Akram, Y. Yen, J. C. Yang, B. Juan, C. Lee, F. Lin, “Wireless power receiver for mobile devices supporting inductive and resonant operating modes”, *IEEE Wireless Power Transfer Conference*, pp. 52 - 55, 2014.
- [67] R. Vyas, H. Nishimoto, M. Tentzeris, Y. Kawahara, T. Asami, “A battery-less, energy harvesting device for long range scavenging of wireless power from terrestrial TV broadcasts”, *IEEE/MTT-S International Microwave Symposium Digest*, pp. 1 - 3, 2012.
- [68] K. Wan, Q. Xue, X. Liu, S. Y. Hui, “Passive Radio-Frequency Repeater for Enhancing Signal Reception and Transmission in a Wireless Charging Platform”, *IEEE Transactions on Industrial Electronics*, vol. 61, pp. 1750 - 1757, 2014.
- [69] M. D. Prete, F. Berra, A. Costanzo, D. Masotti, “Seamless exploitation of cell-phone antennas for near-field WPT by a frequency-diplexing approach”, *IET Microwaves, Antennas & Propagation*, vol. 11, pp. 649 - 656, 2017.
- [70] K. Phaebua, T. Lertwiriayaprapa, C. Phongcharoenpanich, “Study of a repeater Tx

- antenna concept of a portable device wireless battery charging system”, *The 20th Asia-Pacific Conference on Communication (APCC2014)*, pp. 442 - 445, 2014.
- [71] Rajeev Bansal, “The Future of Wireless Charging”, *IEEE Antennas and Propagation Magazine*, vol. 51, pp. 153 - 153, 2009.
- [72] M. Ettorre, W. A. Alomar, A. Grbic, “Long slot Van Atta array for far-field wireless power transfer”, *IEEE International Symposium on Antennas and Propagation & USNC/URSI National Radio Science Meeting*, pp. 1291 - 1293, 2017.
- [73] M. Ettorre, W. A. Alomar, A. Grbic, “Radiative Wireless Power-Transfer System Using Wideband, Wide-Angle Slot Arrays”, *IEEE Transactions on Antennas and Propagation*, vol. 65, pp. 2975 - 2982, 2017.
- [74] L. Gao, Y. Yang, A. Brandon, J. Postma, S. Gong, “Radio frequency wireless power transfer to chip-scale apparatuses”, *IEEE MTT-S International Microwave Symposium (IMS)*, pp. 1-4, 2016.
- [75] Y. Trivedi, “Wireless power transfer: "Look ma, no hands, no wires!", *IEEE Communications Magazine*, vol. 54, pp. 8 - 13, 2016.
- [76] S. Dunbar, F. Wenzl, C. Hack, R. Hafeza, H. Esfeer, F. Defay, S. Prothin, D. Bajon, Z. Popovic, “Wireless far-field charging of a micro-UAV”, *IEEE Wireless Power Transfer Conference (WPTC)*, pp. 1-4, 2015.
- [77] M. Xia, S. Aissa, “On the Efficiency of Far-Field Wireless Power Transfer”, *IEEE Transactions on Signal Processing*, vol. 63, pp. 2835 - 2847, 2015.
- [78] P. D. Hilario Re, S. K. Podilchak, C. Constantinides, G. Goussetis, J. Lee, “An active

- retrodirective antenna element for circularly polarized wireless power transmission”, *IEEE Wireless Power Transfer Conference (WPTC)*, pp. 1-4, 2016.
- [79] V. Singh, A. Kukde, C. Warty, S. Wagh, “Wireless Power Transfer using microstrip antenna assigned with graded index lenses for WSN”, *International Conference on Advances in Computing, Communications and Informatics (ICACCI)*, pp. 1664 - 1669, 2014.
- [80] C. Pani, O. Ray, A. Ghosh, Z. Qadir, M. M. Sarkar, W. Reja, “Wireless power transfer using free space photonics”, *2nd International Conference on Advances in Computing, Communication, & Automation (ICACCA) (Fall)*, pp. 1 - 5, 2016.
- [81] W. P. Choi, W. C. Ho, X. Liu, S. Y. R. Hui, “Bidirectional communication techniques for wireless battery charging systems & portable consumer electronics”, *Twenty-Fifth Annual IEEE Applied Power Electronics Conference and Exposition (APEC)*, pp. 2251 - 2257, 2010.